Fractional SEIRP model for COVID-19 dynamics incorporatingsocial distancing and environment

Saheed Ojo Akindeinde (soakindeinde@oauife.edu.ng)
Obafemi Awolowo University, Nigeria https://orcid.org/0000-0003-2513-1237

E. Okyere
University of Energy and Natural Resources, Ghana

A. O. Adewumi
Obafemi Awolowo University, Nigeria

R. S. Lebelo
Vaal University of Technology, South Africa

O. O. Fabelurin
Obafemi Awolowo University, Nigeria

S. E. Moore
University of Cape Coast, Ghana

Research Article

Keywords: Caputo fractional derivative, covid-19, Banach fixed-point, basic reproduction number, Ulam-Hyers stability, epidemics

Posted Date: February 16th, 2021

DOI: https://doi.org/10.21203/rs.3.rs-244734/v1

Fractional SEIRP model for COVID-19 dynamics incorporating social distancing and environment

S. O. Akindeinde[a]*, E. Okyere[b], A. O. Adewumi [a], R. S. Lebelo [c], O. O. Fabelurin [a] and S. E. Moore [c].

[a] *Department of Mathematics, Obafemi Awolowo University, 220005, Ile-Ife, Nigeria.*

[b] *Department of Mathematics and Statistics, University of Energy and Natural Resources, Ghana.*

[c] *Faculty of Human Sciences, Vaal University of Technology, Vanderbijlpark, South Africa.*

[b] *Department of Mathematics, University of Cape Coast, Cape Coast, Ghana.*

Abstract

We propose a Caputo-based fractional compartmental model for the dynamics of the novel COVID-19 epidemic taking into consideration social distancing and the influence of the environment. Using basic concepts such as continuity and Banach fixed-point theorem, existence and uniqueness of solution to the proposed model was shown. Furthermore, we analyze the stability of the model in the context of Ulam-Hyers and generalized Ulam-Hyers stability criteria. The concept of next-generation matrices was used to compute the basic reproduction number R_0, a number which determines the spread or otherwise of the disease into the general population. Numerical simulation of the disease dynamics was carried out using the fractional Adam-Bashforth-Moulton method to validate the obtained theoretical results.

Keywords: Caputo fractional derivative, covid-19, Banach fixed-point, basic reproduction number, Ulam-Hyers stability, epidemics

1 Introduction

Epidemiological modeling of infectious disease using differential equations with integer-order to examine and investigate the transmission dynamics of epidemics is widely studied in literature [1, 2, 3, 4, 5]. Mathematical modeling of epidemics in literature reveals that nonlinear dynamical equations can give some important insight into the transmission dynamics or dynamical behaviors of disease spread. The recent COVID-19 outbreaks around the world have attracted a lot of interest in the mathematical modeling of this highly contagious disease by constructing realistic nonlinear compartmental mathematical models that are driven by data to better understand the transmission dynamics of the epidemics [6, 7, 8, 9, 10, 11, 12, 13, 14].

Fractional order differential equations are a very useful and powerful mathematical modeling tool to study biological and engineering systems. This is due to the fact that differential operators in these types of equations or models are related to systems with memory dynamics which naturally exists in most biological and engineering systems, see [15, 16, 17]. Differential equations that are characterized by Caputo fractional order derivative have been used to study and analysed several infectious diseases transmission dynamics such as HIV/AIDS [18, 19, 20, 21, 22, 23, 24, 25, 26, 27, 28, 29, 30], TB [31, 32, 33], Malaria [34, 35, 36], Dengue fever [37, 38, 39, 40], Zika [41, 42], Ebola [43, 44, 45] and Hepatitis B [46, 47, 48, 49, 50, 51]. In [52], backward bifurcation dynamics is explored in a basic and realistic vaccination epidemic

*Corresponding Author email: saheed.akindeinde@gmail.com

model. Therein, the author considered rigorous qualitative analysis of the formulated mathematical model and also presented numerical simulations to confirm the obtained theoretical results. [53] [53] extended and studied the cholera epidemic mathematical model formulated by the author in [54] to capture Caputo fractional order derivative. The author in [55] used Lyapunov functions that are of Volterra–type and investigated uniform asymptotic stability of some basic epidemic models (SIS, SIR, SIRS) and the well-known Ross vector-borne diseases in Caputo sense. A 3-compartmental deterministic modeling structure (normal weight-overweight-obese) is constructed to explore obesity epidemic dynamics in a variable population using Caputo fractional-order nonlinear system [56]. The basic SEIR mathematical model driven by Caputo fractional derivative based on the assumption of variable population dynamics is studied in [57]. The authors gave a detailed qualitative stability analysis for their new and realistic deterministic model.

Due to usefulness and powerful nature of fractional order differential equation models in fractional calculus [58, 59, 60, 61, 62], some recent studies in the literature have considered the mathematical modeling of this deadly COVID-19 pandemic using Caputo based nonlinear equations, see [63, 64, 65]. A Caputo fractional-order deterministic epidemic model for COVID-19 infection is developed and studied in [66]. They used the well-known Banach contraction mapping principle to established the existence and uniqueness of the solution for the mathematical model. In a new mathematical modeling study [67], the authors proposed a SEIQRDP fractional-order deterministic model characterized by Caputo derivative to examine the novel coronavirus epidemic. A SEIPAHRF Caputo fractional-order compartmental model is proposed to analyze COVID-19 transmission dynamics in Wuhan [68]. They numerically solved their proposed model and compared it with the initial 67 days reported data on confirmed infected and death cases in Wuhan city. In recent studies, the authors in [69] proposed a Caputo-type nonlinear COVID-19 epidemiological model to explore the significance of lockdown dynamics in controlling the spread of the infectious disease. They further presented the uniqueness and existence of solutions for the mathematical model under lockdown using Banach and Schauder fixed theorems. In [70], a susceptible-exposed-infected-isolated-recovered compartmental modeling framework with constant total population dynamics is used to construct a new SEIQR Caputo fractional-order COVID-19 mathematical model. Owusu-Mensah and co-authors [71], have also studied a new COVID-19 epidemic model using Caputo derivative in fractional calculus. The well-known and powerful generalized form of Adams–Bashforth–Moulton iterative scheme was applied to numerically solve the formulated nonlinear fractional-order differential equation model.

The goal of the present paper is two folds: to establish both the mathematical and biological well-posedness of the integer-order model proposed in [72] and employ an approximate analytical technique to obtain long-term dynamics of the disease. Subsequently, we modify the model to a dimensionally consistent Caputo fractional-order model which has been touted in the literature to describe more efficiently, memory effect typically associated with the way human cells respond to diseases. The paper is organized as follows. Following the essential preliminaries on fractional calculus in Section 2, we examine in Section 3 both mathematical and epidemiological well-posedness of the integer-order model in [72], and obtain disease dynamics using approximate analytical technique proposed in [73], [74]. Section 4 of the paper is devoted to the formulation, well-posedness, local and global stability analysis of the fractional order model. Therein, using basic concepts such as continuity and Banach fixed-point theorem, existence and uniqueness of solution to the proposed model was shown. Furthermore, we discussed stability analysis of the model in the context of Ulam-Hyers and generalized Ulam-Hyers stability criteria. Also, the concept of next-generation matrices was used to compute the basic reproduction number R_0, a number that determines the spread or otherwise of the disease into the general population. We conclude the paper with numerical simulation of the fractional order disease model using

fractional Adam-Bashforth-Moulton; and discussion of results.

2 Preliminaries on fractional calculus

In this section, we introduce well-known definitions and Lemmata in fractional calculus that are relevant for the current article. The interested reader can see the monograph [75] and the article [76] for the proofs and further references.

Definition 2.1. *[75] The fractional order integral of the function $g \in L^1([0,b],\mathbb{R}^+)$ of order $\alpha \in \mathbb{R}^+$ is defined the sense of Riemann-Liouville as*

$$\mathcal{I}^v g(t) = \frac{1}{\Gamma(v)} \int_0^t (t-\tau)^{v-1} g(\tau) d\tau, \quad t > 0$$

where $[0,b] \subset \mathbb{R}^+$ and Γ is the Euler gamma function defined by $\Gamma(v) = \int_0^\infty t^{v-1} e^{-t} dt$, $v > 0$.

Definition 2.2. *[75] For a function $g \in C^n([0,b])$, the Caputo fractional-order derivative of order v of g is defined by*

$$D^v g(t) = \frac{1}{\Gamma(n-v)} \int_0^t (t-\tau)^{n-v-1} g^{(n)}(\tau) d\tau, \quad t > 0$$

where $n = \lfloor v \rfloor + 1$ and $\lfloor v \rfloor$ denotes the smallest integer that is less or equal to v.

Lemma 2.3. *[75] Let $v \geq 0$ and $n = \lfloor v \rfloor + 1$. Then*

$$\mathcal{I}^v (D^v g(t)) = g(t) - \sum_{k=0}^{n-1} \frac{g^k(0)}{k!} t^k.$$

In particular, if $0 < v \leq 1$, then

$$\mathcal{I}^v (D^v g(t)) = g(t) - g_0. \tag{1}$$

Lemma 2.4. *[76] (Generalized Mean Value Theorem) For $0 < v \leq 1$, let $g(t) \in C([a,b])$ and $D^v g(t) \in (a,b]$. Then it holds*

$$g(t) = g(a) + \frac{1}{\Gamma(v)} D^v g(\eta)(t-a)^v, \quad 0 \leq \eta \leq t, \quad \forall\, t \in (a,b].$$

3 Model framework: Integer order model

It is well known that the ravaging Covid-19 virus is transmitted through human-to-human interactions and transmission through the environment. When an infected person sneezes or coughs, the virus is released into the immediate environment which, experts believe, stays viable for as long as five days. We, therefore, consider two interacting populations of humans and pathogens denoted by $N(t)$ and $P(t)$ respectively. At any time t, the total population $N(t)$ is assumed to comprise the susceptible population $S(t)$, the exposed $E(t)$, the asymptomatic infected $I_A(t)$, the symptomatic infected $I_S(t)$ and the recovered population $R(t)$. Thus, $N(t) = S(t) + I_A(t) + I_S(t) + R(t)$. These interactions are depicted in Figure 1 below as reported in [72].

In the figure, b denotes the rate of at which human population is born into susceptible class $S(t)$. The terms $\frac{\beta_1 SP}{1+\alpha_1 P}$ and $\frac{\beta_2 S(I_A+I_S)}{1+\alpha_2(I_A+I_S)}$ represent rate at which the susceptible get infected by pathogens and through interactions with infectious asymptomatic $I_A(t)$ and infectious symptomatic $I_S(t)$. The denominators in the above terms factor in the adherence to recent experts advice on social distancing and the use of face masks which minimizes contact with infectious individuals, and transmission through the environment.

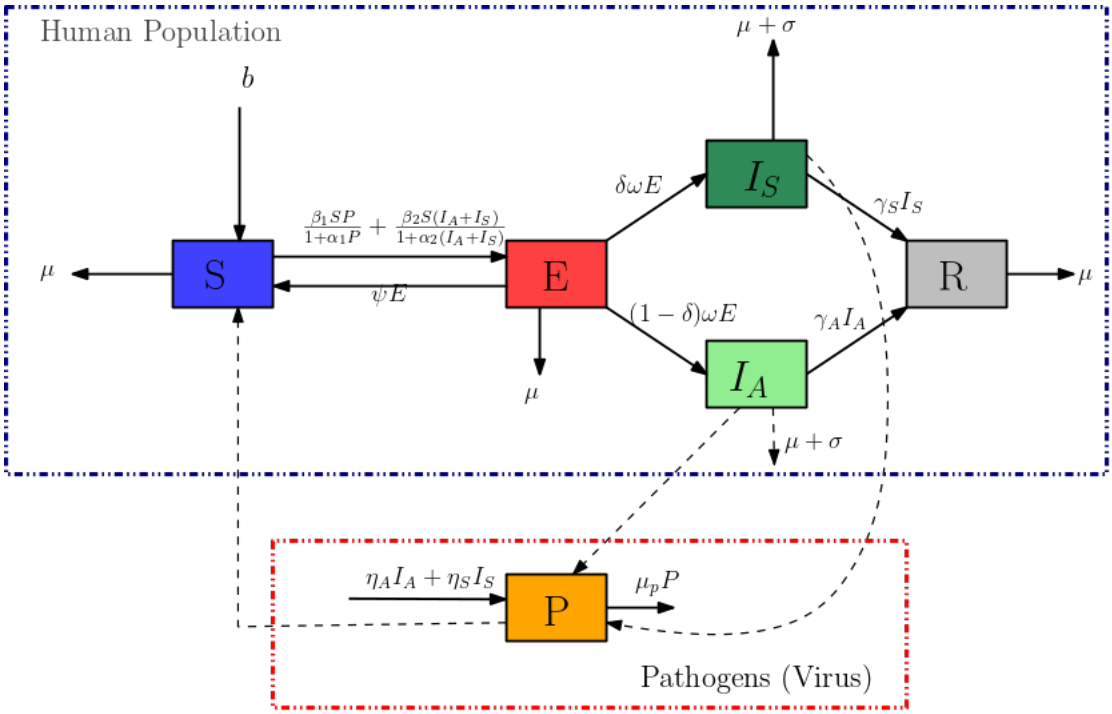

Figure 1: The SEIR-P model for COVID-19 disease dynamics

Based on the above description, the authors in [72] proposed the following integer-order differential equation to model the dynamics of the transmission of covid-19 taking into account environment and social distancing, namely

$$\begin{aligned}
S'(t) &= b - \frac{\beta_1 SP}{1+\alpha_1 P} - \frac{\beta_2 S(I_A+I_S)}{1+\alpha_2(I_A+I_S)} + \psi E - \mu S,\\
E'(t) &= \frac{\beta_1 SP}{1+\alpha_1 P} + \frac{\beta_2 S(I_A+I_S)}{1+\alpha_2(I_A+I_S)} - \psi E - \mu E - \omega E,\\
I_A'(t) &= (1-\delta)\omega E - (\mu+\sigma)I_A - \gamma_A I_A,\\
I_S'(t) &= \delta\omega E - (\mu+\sigma)I_S - \gamma_S I_S,\\
R'(t) &= \gamma_S I_S + \gamma_A I_A - \mu R,\\
P'(t) &= \eta_A I_A + \eta_S I_S - \mu_p P
\end{aligned} \tag{2}$$

with initial conditions $S(0) = S_0 > 0$, $E(0) = E_0 > 0$, $I_A(0) = I_{A0} > 0$, $I_S(0) = I_{S0} > 0$, $R(0) = R_0 > 0$ Therein, the authors analysed the equilibra and basic reproduction number of the model, and numerical simulation. However, the analysis in article [72] did not examine the essential well-posedness of the proposed model. Here in the present paper, for completeness, we begin our exposition by establishing qualitative properties of the integer order model which ensures that the model is both mathematically and epidemiological well-posed i.e. existence, uniqueness, positivity and boundedness of the solutions to the model. Furthermore, establishing the aforementioned properties allows us the extend the study in [72] to fractional order model, which accommodate the memory effect typically associated with epidemic disease models. In addition, we shall obtain approximate analytical solutions of the model via a multistage method proposed in [73], [74].

3.0.1 Well-posedness

For the fact that (2) models human populations, all the model parameters are assumed non-negative, see Table 1 for values and description of the model parameters. It then remains to

Table 1: Model parameters and their descriptions [72]

Parameter description	**Symbol**	**Value**
Birth rate of the human population	b	0.00018 days^{-1}
Natural human death rate	μ	4.563×10^{-5}days^{-1}
Human life expectancy	$1/\mu$	21915 days or 60ye
Natural death rate of pathogens in the environment	μ_p	0.1724 days^{-1}
Life expectancy of pathogens in the environment	$1/\mu_p$	5.8 days
Proportion of interaction with an infectious environment	α_1	0.10
Proportion of interaction with an infectious individual	α_2	0.10
Rate of transmission from S to E due to contact with P	β_1	0.00414
Rate of transmission from S to E due to contact with I_A and/or I_S	β_2	0.0115
Proportion of symptomatic infectious people	δ	0.7
Progression rate from E back to S due to robust immune system	ψ	0.0051
Progression rate from E to either I_A or I_S	ω	0.09
Death rate due to the coronavirus	σ	0.0018
Rate of recovery of the symptomatic population	γ_S	0.05days^{-1}
Rate of recovery of the asymptomatic human population	γ_A	0.0714days^{-1}
Rate of virus spread to environment by symptomatic infectious individuals	η_S	0.1days^{-1}
Rate of virus spread to environment by asymptomatic infectious individuals	η_A	0.1days^{-1}

show that unique solution exists for the model and that the state variables remain bounded and non-negative for all time $t > 0$.

Theorem 3.1. *(Existence and uniqueness of solution) Let $t_f \in \mathbb{R}^+$. The dynamical system (2) admits a unique solution on interval $(0, t_f)$ for initial conditions satisfying $S(0) > 0$, $E(0) > 0$, $I_A(0) > 0$, $I_S(0) > 0$, $R(0) > 0$, $P(0) > 0$.*

Proof. By defining $y(t) = (S(t), E(t), I_A(t), I_S(t), R(t), P(t))^T$, then (2) can be written as $y'(t) = F(y(t)) = (f_1, f_2, f_3, f_4, f_5, f_6)^T$ where the f_i are functions of $y(t)$. By assumption the initial condition $y(0) = (S(0), E(0), I_A(0), I_S(0), R(0), P(0))^T > 0$. Thus computing and examining the entries of the Jacobian $J(F(y))$, e.g.

$$J_{11} = \frac{\partial f_1}{\partial S} = \frac{\beta_1 P}{1+\alpha_1 P} - \frac{\beta_2(I_A+I_S)}{1+\alpha_2(I_A+I_S)} - \mu, \quad J_{12} = \frac{\partial f_1}{\partial E} = \psi$$

$$J_{13} = \frac{\partial f_1}{\partial I_A} = -\frac{-\beta_2 S}{\Big(1+\alpha_2(I_A+I_S)\Big)^2} = J_{14} = \frac{\partial f_1}{\partial I_S}, \quad J_{15} = \frac{\partial f_1}{\partial R} = 0$$

$$J_{16} = \frac{\partial f_1}{\partial P} = -\frac{\beta_1 S}{(1+\alpha_1 P)^2}, \quad \text{etc}$$

reveal that both the right hand side of (2) namely F and its Jacobian are continuous for $t > 0$. Thus, F satisfies a Lipschitz condition on $\mathbb{R}^6_+$. The existence and uniqueness of solution for some time interval $(0, t_f)$ follows from Picard-Lindelof Theorem. □

Theorem 3.2. *(Positivity of solution) The state variables $S(t), E(t), I_A(t), I_S(t), R(t), P(t)$ of (2) with non-negative initial data remains non-negative for all $t > 0$.*

Proof. Let $S(0) = S_0 > 0$. It follows from the first equation of (2) that

$$\frac{\mathrm{d}S}{\mathrm{d}t} \geq -\Big(\frac{\beta_1 P}{1+\alpha_1 P} + \frac{\beta_2(I_A+I_S)}{1+\alpha_2(I_A+I_S)} + \mu\Big)S$$

and upon integration, one obtains

$$S(t) \geq S_0 e^{-(\mu t+\delta)} > 0 \tag{3}$$

for all $t > 0$ where

$$\delta = \int_0^t \Big(\frac{\beta_1 P(\tau)}{1+\alpha_1 P(\tau)} + \frac{\beta_2 (I_A(\tau)+I_S(\tau))}{1+\alpha_2 (I_A(\tau)+I_S(\tau))} \Big) \mathrm{d}\tau.$$

Similar arguments yield

$$\begin{aligned} E(t) &\geq E(0) e^{-(\psi+\mu+\omega)t} > 0 \\ I_A(t) &\geq I_A(0) e^{-(\mu+\sigma+\gamma_A)t} > 0 \\ I_S(t) &\geq I_S(0) e^{-(\psi+\mu+\gamma_S)t} > 0 \\ R(t) &\geq R(0) e^{-\mu t} > 0 \\ P(t) &\geq P(0) e^{-\mu_p t} > 0 \end{aligned}$$

and as a consequence, non-negativity of the remaining state variables are obtained. □

Theorem 3.3. *(Boundedness of solution) The integer order model* (2) *has solutions bounded within invariant region given by*

$$\Omega = \Big\{ (S, E, I_A, I_S, R, P) \in \mathbb{R}^6 : 0 \leq N(t) \leq \frac{b}{\mu},\ 0 \leq P(t) \leq \frac{\eta\, b}{\mu\, \mu_p} \Big\}$$

where $\eta = \eta_A + \eta_S$.

Proof. Using the fact that $N(t) = S(t) + E(t) + I_A(t) + I_S(t) + R(t)$, it follows from (2) that

$$\begin{aligned} N'(t) &= b - (\mu+\sigma)(I_A + I_S) - \mu(R + S + E) \\ &= b - \mu N - \sigma(I_A + I_S) \\ &\leq b - \mu N. \end{aligned}$$

Thus considering the initial valued problem $N'(t) = b - \mu N, \quad N(0) = N_0$ and invoking comparison theorem [77], it follows that

$$N(t) \leq N_0 e^{-\mu t} + \frac{b}{\mu}(1 - e^{-\mu t})$$

and consequently

$$\limsup_{t\to\infty} N(t) \leq \frac{b}{\mu}.$$

For the pathogen population, using the fact that $I_A + I_S \leq N \leq b/\mu$, the last equation of (2) yields

$$\begin{aligned} P'(t) &= \eta_A I_A + \eta_S I_S - \mu_p P \\ &\leq \eta(I_A + I_S) - \mu_p P, \qquad \eta = \eta_A + \eta_S \\ &\leq \eta\, \frac{b}{\mu} - \mu_p P \end{aligned}$$

and consequently $P(t) \leq P_0 e^{-\mu_p t} + \frac{\eta\, b}{\mu\, \mu_p}(1 - e^{-\mu_p t})$. Thus $\limsup_{t\to\infty} P(t) \leq \frac{\eta\, b}{\mu\, \mu_p}$. □

3.0.2 Approximate analytical solution of the integer order model

Here, we shall adopt the multistage technique proposed in [73], [74] to compute approximate analytical solution to the integer order model (2). For that purpose, let us define $U = \frac{1}{1+\alpha_1 P}$ and $W = \frac{1}{1+\alpha_2(I_A+I_S)}$ so that (2) is transformed to an equivalent polynomial system

$$\begin{aligned}
S'(t) &= b - \beta_1 SPU - \beta_2 S(I_A + I_S)W + \psi E - \mu S,\\
E'(t) &= \beta_1 SPU + \beta_2 S(I_A + I_S)W - \psi E - \mu E - \omega E,\\
I_A'(t) &= (1-\delta)\omega E - (\mu+\sigma)I_A - \gamma_A I_A,\\
I_S'(t) &= \delta\omega E - (\mu+\sigma)I_S - \gamma_S I_S,\\
R'(t) &= \gamma_S I_S + \gamma_A I_A - \mu R,\\
P'(t) &= \eta_A I_A + \eta_S I_S - \mu_p P.\\
U'(t) &= -\alpha_1 U^2(\eta_A I_A + \eta_S I_S - \mu_p P)\\
W'(t) &= -\alpha_2 W^2\Big(\omega E - (\mu+\sigma)(I_A+I_S) - \gamma_A I_A - \gamma_S I_S\Big)
\end{aligned} \tag{4}$$

which is now amenable to the proposed technique. By writing $S(t) = \sum_{n=0}^{\infty} S_n t^n$, it follows from the above polynomial system that the coefficients S_n are obtained recursively through

$$(n+1)S_n = b - \beta_1 (SPU)_n - \beta_2\Big(S(I_A+I_S)W\Big)_n + \psi E_n - \mu S_n, \quad S_0 = S(0).$$

In a similar manner, approximate analytical solutions of the remaining compartments are computed. Such series solution often have small interval of convergence. Therefore to improve convergence, we choose a safe step length h, (see [73] and [74]) and compute a piecewise continuous approximate solution which is convergent in the entire integration interval. The dynamics of the disease progression for each sub-population are displayed in Figures 2a-2d and Figures 3a-3b below, confirming the results in [72].

4 Fractional order model

Fractional derivative are generally believed to model disease epidemic more realistically because of their capability to capture memory effect often associated with human body response to diseases. Here, we propose a fractional order variant of (2) given by

$$\begin{aligned}
D_t^\alpha S(t) &= b^\alpha - \frac{\beta_1^\alpha SP}{1+\alpha_1 P} - \frac{\beta_2^\alpha S(I_A+I_S)}{1+\alpha_2(I_A+I_S)} + \psi^\alpha E - \mu^\alpha S,\\
D_t^\alpha E(t) &= \frac{\beta_1^\alpha SP}{1+\alpha_1 P} + \frac{\beta_2^\alpha S(I_A+I_S)}{1+\alpha_2(I_A+I_S)} - \psi^\alpha E - \mu^\alpha E - \omega^\alpha E,\\
D_t^\alpha I_A(t) &= (1-\delta)\omega^\alpha E - (\mu^\alpha+\sigma^\alpha)I_A - \gamma_A^\alpha I_A,\\
D_t^\alpha I_S(t) &= \delta\omega^\alpha E - (\mu^\alpha+\sigma^\alpha)I_S - \gamma_S^\alpha I_S,\\
D_t^\alpha R(t) &= \gamma_S^\alpha I_S + \gamma_A^\alpha I_A - \mu^\alpha R,\\
D_t^\alpha P(t) &= \eta_A^\alpha I_A + \eta_S^\alpha I_S - \mu_p^\alpha P
\end{aligned} \tag{5}$$

subject to initial conditions $S(0) = S_0 > 0$, $E(0) = E_0 > 0$, $I_A(0) = I_{A0} > 0$, $I_S(0) = I_{S0} > 0$, $R(0) = R_0 > 0$. In the above, operator D^α denotes Caputo fractional derivative of order $0 < \alpha \leq 1$. Noting that all the model parameters except α_1, α_2 and δ have dimensions $1/t^\alpha$, we have raised these parameters to power of α for dimensional consistency emphasized by [38].

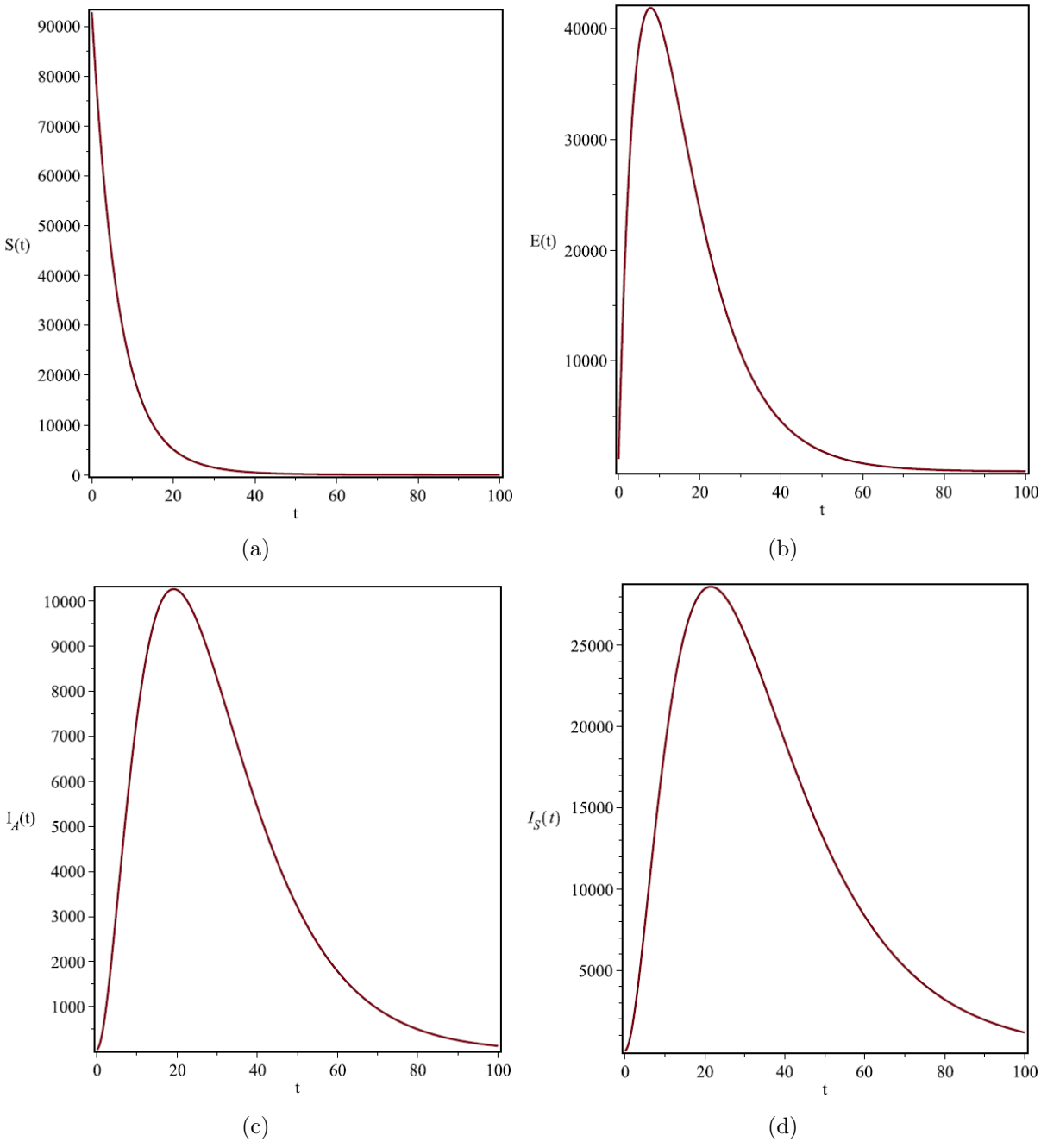

Figure 2: Disease dynamics of the integer-order model.

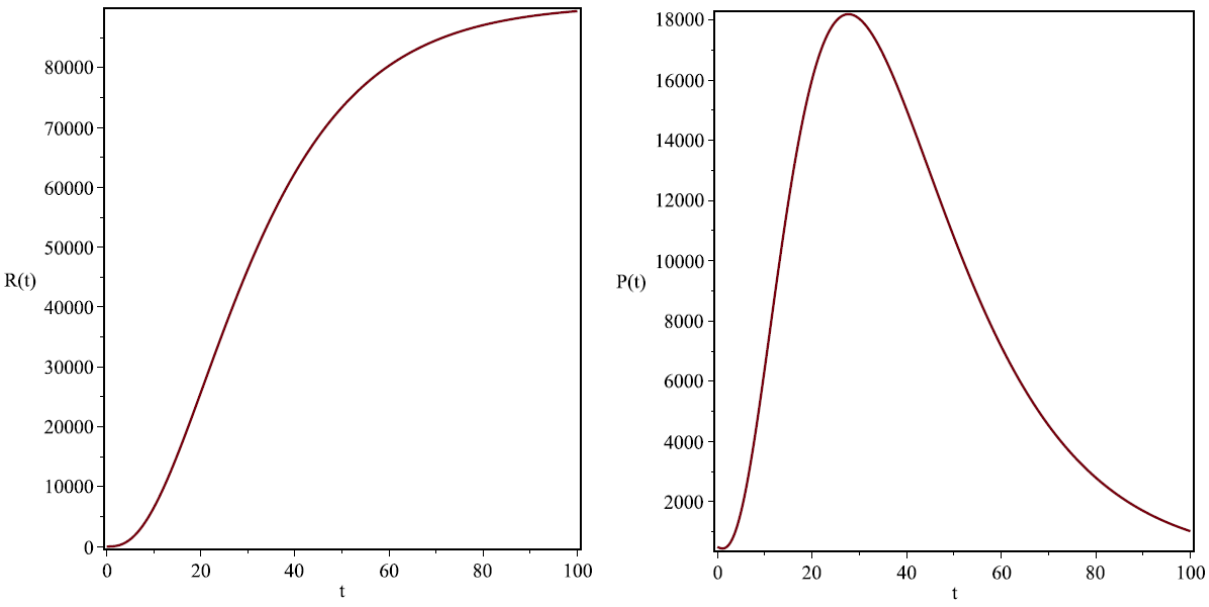

(a) (b)

Figure 3: Disease dynamics of the integer-order model.

4.1 Qualitative properties of solution

In this section, we examine the mathematical and biological well-posedness of the fractional order model. In essence, we prove that solution of the fractional model is bounded and remains positive as long as a positive initial condition is given. Furthermore, we prove the existence and uniqueness of the solution to the modified model.

Let $X(t) = (S, E, I_A, I_S, R, P)^T$ and $\mathcal{K}(t, X(t)) = (\phi_i)^T,\ i = 1, 2, \ldots 6$ where

$$\begin{aligned}
\phi_1 &= b^\alpha - \frac{\beta_1^\alpha SP}{1+\alpha_1 P} - \frac{\beta_2^\alpha S(I_A+I_S)}{1+\alpha_2(I_A+I_S)} + \psi^\alpha E - \mu^\alpha S \\
\phi_2 &= \frac{\beta_1^\alpha SP}{1+\alpha_1 P} + \frac{\beta_2^\alpha S(I_A+I_S)}{1+\alpha_2(I_A+I_S)} - \psi^\alpha E - \mu^\alpha E - \omega^\alpha E \\
\phi_3 &= (1-\delta)\omega^\alpha E - (\mu^\alpha + \sigma^\alpha) I_A - \gamma_A^\alpha I_A, \\
\phi_4 &= \delta\omega^\alpha E - (\mu^\alpha + \sigma^\alpha) I_S - \gamma_S^\alpha I_S, \\
\phi_5 &= \gamma_S^\alpha I_S + \gamma_A^\alpha I_A - \mu^\alpha R, \\
\phi_6 &= \eta_A^\alpha I_A + \eta_S^\alpha I_S - \mu_p^\alpha P.
\end{aligned}$$

Then the dynamical system (5) can be written as

$$D_t^\alpha X(t) = \mathcal{K}(t, X(t)), \quad X(0) = X_0 \geq 0, \quad t \in [0, b], \quad 0 < \alpha \leq 1. \tag{6}$$

In the above, the condition $X(0) \geq 0$ is to be interpreted component-wise. Problem (6), which is equivalent to fractional differential equation (5), in turn has integral representation

$$\begin{aligned}
X(t) &= X_0 + \mathcal{J}_{0^+}^\alpha \mathcal{K}(t, X(t)) \\
&= X_0 + \frac{1}{\Gamma(\alpha)} \int_0^t (t-\tau)^{\alpha-1} \mathcal{K}(\tau, X(\tau)) \mathrm{d}\tau
\end{aligned} \tag{7}$$

Next, we shall analyse model (5) through the integral representation above. For that purpose, let $\mathcal{E} = C([0, b]; \mathbb{R})$ denote the Banach space of all continuous functions from $[0, b]$ to $\mathbb{R}$ endowed with the norm

$$||X||_{\mathcal{E}} = \sup_{t \in [0,b]} \{|X(t)|\}$$

where $|X(t)| = |S(t)| + |E(t)| + |I_A(t)| + |I_S(t)| + |R(t)| + |P(t)|$. Note that S, E, I_A, I_S, R, P all belong to $C([0, b]; \mathbb{R})$. Furthermore, we define the operator $P : \mathcal{E} \to \mathcal{E}$ by

$$(PX)(t) = X_0 + \frac{1}{\Gamma(\alpha)} \int_0^t (t-\tau)^{\alpha-1} \mathcal{K}(\tau, X(\tau)) \mathrm{d}\tau. \tag{8}$$

Note that operator P is well-defined due to obvious continuity of $\mathcal{K}$.

4.1.1 Positivity and boundedness of solution

For the fractional order model to be biologically well-posed, its solution is expected to be positive and bounded at all times. These properties are established in the sequel.

Theorem 4.1. *Let $X(t) = (S, E, I_A, I_S, R, P)^T$. Then for $X(0) > 0$, the solution $X(t)$ of (5) is bounded, and remains positive for $t \geq 0$.*

Proof. We start by establishing positiveness of solution. Following [78], consider the trajectory of solution along the S-axis where $E(0) = I_A(0) = I_S(0) = R(0) = P(0)$, and $S(0) = S_0 > 0$. Then $D_t^\alpha S(t) = b^\alpha - \mu^\alpha S, \quad S(0) = S_0$ whose solution is given by $S(t) = S_0 E_\alpha(-\mu^\alpha t^\alpha) + \frac{b^\alpha}{\mu^\alpha}(1 - E_\alpha(-\mu^\alpha t^\alpha)) > 0$. Since $E(0) > 0, I_A(0) > 0, I_S(0) > 0, R(0) > 0, P(0)$, similar arguments yield

$$\begin{aligned}
E(t) &= E(0) E_\alpha(-(\psi^\alpha + \mu^\alpha + \omega^\alpha) t^\alpha) > 0 \\
I_A(t) &= I_A(0) E_\alpha(-(\mu^\alpha + \sigma^\alpha + \gamma_A^\alpha) t^\alpha) > 0 \\
I_S(t) &= I_S(0) E_\alpha(-(\psi^\alpha + \mu^\alpha + \gamma_S^\alpha) t^\alpha) > 0 \\
R(t) &= R(0) E_\alpha(-\mu^\alpha t^\alpha) > 0 \\
P(t) &= P(0) E_\alpha(-\mu_p^\alpha t^\alpha) > 0
\end{aligned}$$

showing non-negative invariance of the axes.

Now, since the solution to the model (5) is positive in the $E - I_A - I_S - R - P$ plane, let $t^* > 0$ such that $S(t^*) = 0, E(t^*) > 0, I_A(t^*) > 0, I_S(t^*) > 0, R(t^*) > 0, P(t^*) > 0$ and $S(t) < S(t^*)$. On this plane,

$$D_t^\alpha S(t)\Big|_{t=t^*} = b^\alpha > 0 \tag{9}$$

By Caputo fractional mean value theorem (see Lemma 2.4), it holds $S(t) - S(t^*) = \frac{1}{\Gamma(\alpha)} D_t^\alpha(\tau)(t - t^*)^\alpha$, $\tau \in [t^*, t)$. Therefore, using (9), we obtain $S(t) > S(t^*)$, contradicting our earlier assumption for t^*. Thus, any solution $S(t)$ is non-negative for all $t \geq 0$. The remaining variables can be treated similarly. Hence, solution $X(t)$ remains positive for all $t \geq 0$.

Finally for boundedness, proceeding as in the integer order case (see the proof of Theorem 3.3), one obtains $N(t) \leq N_0 E_\alpha(-\mu^\alpha t^\alpha) + \frac{b^\alpha}{\mu^\alpha}(1 - E_\alpha(-\mu^\alpha t^\alpha))$ and consequently $\limsup_{t\to\infty} N(t) \leq \frac{b^\alpha}{\mu^\alpha}$. Similarly, $\limsup_{t\to\infty} P(t) \leq \frac{\eta^\alpha b^\alpha}{\mu^\alpha \mu_p^\alpha}$.

□

4.1.2 Existence of unique and uniformly stable solution

Here, we establish existence, uniqueness and uniform stability of solutions to (4) through (5). The following preliminary result is in order.

Lemma 4.2. *Let $\bar{X} = (\bar{S}, \bar{E}, \bar{I_A}, \bar{I_S}, \bar{R}, \bar{P})^T$. The function $\mathcal{K} = (\phi_i)^T$ defined above satisfies*

$$||\mathcal{K}(t, X(t)) - \mathcal{K}(t, \bar{X}(t))||_{\mathcal{E}} \leq L_{\mathcal{K}} ||X - \bar{X}||_{\mathcal{E}}$$

for some $L_{\mathcal{K}} > 0$.

Proof. From the first component of $\mathcal{K}$, we observe that

$$\begin{aligned}
&|\phi_1(t,X(t)) - \phi_1(t,\bar{X}(t))| \\
&\quad = \Big|\beta_1^\alpha\Big(\frac{S(t)P(t)}{1+\alpha_1 P(t)} - \frac{\bar{S}(t)\bar{P}(t)}{1+\alpha_1\bar{P}(t)}\Big) - \beta_2^\alpha\Big(\frac{S(t)(I_A(t)+I_S(t))}{1+\alpha_2(I_A(t)+I_S(t))} - \frac{\bar{S}(t)(\bar{I}_A(t)+\bar{I}_S(t))}{1+\alpha_2(\bar{I}_A(t)+\bar{I}_S(t))}\Big) \\
&\qquad + \psi^\alpha(E(t)-\bar{E}(t)) - \mu^\alpha(S(t)-\bar{S}(t))\Big| \\
&\quad \le \beta_1^\alpha\Big|\frac{S(t)P(t)}{1+\alpha_1 P(t)} - \frac{\bar{S}(t)\bar{P}(t)}{1+\alpha_1\bar{P}(t)}\Big| + \beta_2^\alpha\Big|\frac{S(t)(I_A(t)+I_S(t))}{1+\alpha_2(I_A(t)+I_S(t))} - \frac{\bar{S}(t)(\bar{I}_A(t)+\bar{I}_S(t))}{1+\alpha_2(\bar{I}_A(t)+\bar{I}_S(t))}\Big| \\
&\qquad + \psi^\alpha|E(t)-\bar{E}(t)| + \mu^\alpha|S(t)-\bar{S}(t)|.
\end{aligned}$$

However,

$$\begin{aligned}
\Big|\frac{S(t)P(t)}{1+\alpha_1 P(t)} - \frac{\bar{S}(t)\bar{P}(t)}{1+\alpha_1\bar{P}(t)}\Big| &= \Big|\frac{S(t)P(t)(1+\alpha_1\bar{P}(t)) - \bar{S}(t)\bar{P}(t)(1+\alpha_1 P(t))}{(1+\alpha_1 P(t))(1+\alpha_1\bar{P}(t))}\Big| \\
&\le f_1(t)|S(t)-\bar{S}(t)| + f_2(t)|P(t)-\bar{P}(t)|
\end{aligned}$$

where

$$f_1(t) = |P(t)| + \alpha_1|P(t)||\bar{P}(t)|, \quad f_2(t) = |\bar{S}(t)|$$

Similarly we obtain,

$$\begin{aligned}
&\Big|\frac{S(t)(I_A(t)+I_S(t))}{1+\alpha_2(I_A(t)+I_S(t))} - \frac{\bar{S}(t)(\bar{I}_A(t)+\bar{I}_S(t))}{1+\alpha_2(\bar{I}_A(t)+\bar{I}_S(t))}\Big| \\
&\qquad\qquad \le g_1(t)|S(t)-\bar{S}(t)| + g_2(t)|I_A(t)-\bar{I}_A(t)| + g_3(t)|I_S(t)-\bar{I}_S(t)|
\end{aligned}$$

where

$$g_1(t) = |I_A(t) + \alpha_2 I_A(t)\bar{I}_A(t) + \alpha_2\bar{I}_A(t)I_S(t)|,\ g_2(t) = |\bar{S}(t) + \alpha_2 S(t)\bar{I}_S(t)|,\ g_3(t) = |\alpha_2\bar{I}_A(t)S(t)|.$$

Altogether, we have

$$\begin{aligned}
|\phi_1(t,X(t)) - \phi_1(t,\bar{X}(t))| &\le (\mu^\alpha + \beta_1^\alpha f_1(t) + \beta_2^\alpha g_1(t))|S(t)-\bar{S}(t)| + \psi^\alpha|E(t)-\bar{E}(t)| \\
&\quad + \beta_2^\alpha g_2(t)|I_A(t)-\bar{I}_A(t)| + \beta_2^\alpha g_3(t)|I_S(t)-\bar{I}_S(t)| + \beta_1^\alpha f_2(t)|P(t)-\bar{P}(t)| \\
&\le L_1\Big(|S(t)-\bar{S}(t)| + |E(t)-\bar{E}(t)| + |I_A(t)-\bar{I}_A(t)| + |I_S(t)-\bar{I}_S(t)| \\
&\quad + |P(t)-\bar{P}(t)|\Big)
\end{aligned}$$

where

$$L_1 = \mu^\alpha + \psi^\alpha + \max_{t\in[0,b]}\{\beta_1^\alpha f_1(t) + \beta_1^\alpha f_2(t) + \beta_2^\alpha g_1(t) + \beta_2^\alpha g_2(t) + \beta_1^\alpha g_3(t)\}.$$

In a similar manner, one obtains

$$\begin{aligned}
|\phi_2(t,X(t)) - \phi_2(t,\bar{X}(t))| \le L_1\Big(&|S(t)-\bar{S}(t)| + |E(t)-\bar{E}(t)| + |I_A(t)-\bar{I}_A(t)| + |I_S(t)-\bar{I}_S(t)| \\
&+ |P(t)-\bar{P}(t)|\Big)
\end{aligned}$$

where

$$L_2 = \mu^\alpha + \psi^\alpha + \omega^\alpha + \max_{t\in[0,b]}\{\beta_1^\alpha f_1(t) + \beta_1^\alpha f_2(t) + \beta_2^\alpha g_1(t) + \beta_2^\alpha g_2(t) + \beta_1^\alpha g_3(t)\}.$$

For the remaining components of $\mathcal{K}$, it holds

$$
\begin{aligned}
|\phi_3(t,X(t)) - \phi_3(t,\bar{X}(t))| &\leq L_3\Big(|E(t)-\bar{E}(t)| + |I_A(t)-\bar{I}_A(t)|\Big)\\
|\phi_4(t,X(t)) - \phi_4(t,\bar{X}(t))| &\leq L_4\Big(|E(t)-\bar{E}(t)| + |I_A(t)-\bar{I}_A(t)|\Big)\\
|\phi_5(t,X(t)) - \phi_5(t,\bar{X}(t))| &\leq L_5\Big(|I_A(t)-\bar{I}_A(t)| + |I_S(t)-\bar{I}_S(t)| + |R(t)-\bar{R}(t)|\Big)\\
|\phi_6(t,X(t)) - \phi_6(t,\bar{X}(t))| &\leq L_6\Big(|I_A(t)-\bar{I}_A(t)| + |I_S(t)-\bar{I}_S(t)| + |P(t)-\bar{P}(t)|\Big)
\end{aligned}
$$

with $L_3 = |1-\delta|\omega^\alpha+\mu^\alpha+\sigma^\alpha+\gamma_A^\alpha,\ L_4 = \delta\omega^\alpha+\mu^\alpha+\sigma^\alpha+\gamma_S^\alpha,\ L_5 = \gamma_S^\alpha+\gamma_A^\alpha+\mu^\alpha,\ L_6 = \eta_A^\alpha+\eta_S^\alpha+\mu_p^\alpha$. Consequently,

$$
\begin{aligned}
||\mathcal{K}(t,X(t)) - \mathcal{K}(t,\bar{X}(t))||_{\mathcal{E}} &= \sup_{t\in[0,b]}\sum_{i=1}^{6}|\phi_i(t,X(t)) - \phi_i(t,\bar{X}(t))|\\
&\leq L_{\mathcal{K}}||X-\bar{X}||_{\mathcal{E}}
\end{aligned}
$$

where $L_{\mathcal{K}} = L_1+L_2+L_3+L_4+L_5+L_6$. □

Theorem 4.3. *Let the result of Lemma 4.2 holds and* $\Omega = \frac{b^v}{\Gamma(v+1)}$. *If* $\Omega L_{\mathcal{K}} < 1$, *then there exists a unique solution of model* (5) *on* $[0,b]$ *which is uniformly Lyapunov stable.*

Proof. The function $\mathcal{K} : [0,b]\times\mathbb{R}^6 \to \mathbb{R}_+^6$ is clearly continuous on its domain. Thus, existence of solution to (5) follows from [79, Theorem 3.1].

For uniqueness, we shall use Banach contraction mapping principle on operator P defined in (8) above. For that purpose, we show that P is both a self map and a contraction. Firstly, by definition, $\sup_{t\in[0,b]}||\mathcal{K}(t,0)|| = b^v$. Let us now define $\kappa > \frac{||X_0||+\Omega b^v}{1-\Omega L_{\mathcal{K}}}$ and a closed convex set $B_\kappa = \{X\in\mathcal{E} : ||X||_{\mathcal{E}} \leq \kappa\}$. Thus for self map property, it suffices to show that $PB_\kappa \subseteq B_\kappa$. So, let $X\in B_\kappa$, then

$$
\begin{aligned}
||PX||_{\mathcal{E}} &= \sup_{t\in[0,b]}\Big\{\Big|X_0 + \frac{1}{\Gamma(v)}\int_0^t (t-\tau)^{v-1}\mathcal{K}(\tau,X(\tau))\mathrm{d}\tau\Big|\Big\}\\
&\leq |X_0| + \frac{1}{\Gamma(v)}\sup_{t\in[0,b]}\Big\{\int_0^t (t-\tau)^{v-1}\Big(\Big|\mathcal{K}(\tau,X(\tau)) - \mathcal{K}(\tau,0)\Big| + \Big|\mathcal{K}(\tau,0)\Big|\Big)\mathrm{d}\tau\Big\}\\
&\leq |X_0| + \frac{1}{\Gamma(v)}\sup_{t\in[0,b]}\Big\{\int_0^t (t-\tau)^{v-1}\Big(||\mathcal{K}(\tau,X(\tau)) - \mathcal{K}(\tau,0)||_{\mathcal{E}} + ||\mathcal{K}(\tau,0)||_{\mathcal{E}}\Big)\mathrm{d}\tau\Big\}\\
&\leq |X_0| + \frac{L_{\mathcal{K}}||X||_{\mathcal{E}} + b^v}{\Gamma(v)}\sup_{t\in[0,b]}\Big\{\int_0^t (t-\tau)^{v-1}\mathrm{d}\tau\Big\}\\
&\leq |X_0| + \frac{L_{\mathcal{K}}\kappa + b^v}{\Gamma(v)}\sup_{t\in[0,b]}\Big\{\int_0^t (t-\tau)^{v-1}\mathrm{d}\tau\Big\}\\
&= |X_0| + \frac{L_{\mathcal{K}}\kappa + b^v}{\Gamma(v+1)}b^v\\
&= |X_0| + \Omega(L_{\mathcal{K}}\kappa + b^v)\\
&\leq \kappa.
\end{aligned}
$$

□

It then follows that operator $PX \subseteq B_\kappa$ and P is indeed a self-map. It remains at this point to prove that P is a contraction. Let X and $\tilde{X}\in\mathcal{E}$ satisfy (6). Then again using the result of

Lemma 4.2 we have

$$\begin{aligned}||PX - P\tilde{X}||_{\mathcal{E}} &= \sup_{t\in[0,b]}\Big\{|(PX)(t) - (P\tilde{X})(t)|\Big\}\\ &= \frac{1}{\Gamma(v)}\sup_{t\in[0,b]}\Big\{\int_0^t (t-\tau)^{v-1}|\mathcal{K}(\tau, X(\tau)) - \mathcal{K}(\tau,\tilde{X}(\tau))|\mathrm{d}\tau\Big\}\\ &\leq \frac{L_{\mathcal{K}}}{\Gamma(v)}\sup_{t\in[0,b]}\Big\{\int_0^t (t-\tau)^{v-1}|X(\tau) - \tilde{X}(\tau)|\mathrm{d}\tau\Big\}\\ &\leq \Omega L_{\mathcal{K}}||X - \tilde{X}||_{\mathcal{E}}.\end{aligned}$$

Thus if $\Omega L_{\mathcal{K}} < 1$ then P is a contraction mapping, and consequently by the Banach contraction mapping principle, P has a unique fixed point on $[0, b]$ which is solution of (5). Uniformly Lyapunov stability of solution follows from [80, Theorem 3.2].

4.2 Equilibra and Basic reproduction number of the fractional order model

By setting the left hand side of (5) to zero, one obtains the equilbra points. Disease-free equilibrium points are those where $I_A = I_S = 0$ and $P = 0$. These immediately imply $E = 0$ and $R = 0$. Thus, we obtain $b^\alpha - \mu^\alpha S^* = 0$ or $S^* = b^\alpha/\mu^\alpha$. Consequently, the disease-free equilibrium point of the fractional-order model is $(S^*, E^*, I_A^*, I_S^*, R^*, P^*) = (\frac{b^\alpha}{\mu^\alpha}, 0, 0, 0, 0, 0)$.

The dynamic and stability of a disease model is usually governed by the basic reproduction number R_0 which simply put, measure the average number of secondary infections resulting from introducing one infected individual into an entirely susceptible population. In other words, it determines the spread or otherwise of the infection into the entire population. We follow the recipes described in [81] to compute the basic reproduction number for the fractional order model. The approach is based on next-generation matrices.

The infected subsystem of (5) comprises the second, third, fourth and sixth equations. Therefore, letting $x = (E, I_A, I_S, P)^T$, then the infected subsystem can be written in the form $x'(t) = \mathcal{F}(x) - \mathcal{V}(x)$ where

$$\mathcal{F}(x) = \begin{pmatrix} \frac{\beta_1^\alpha SP}{1+\alpha_1 P} + \frac{\beta_2^\alpha S(I_A+I_S)}{1+\alpha_2(I_A+I_S)} \\ 0 \\ 0 \\ \eta_A^\alpha I_A + \eta_S^\alpha I_S \end{pmatrix}, \qquad \mathcal{V}(x) = \begin{pmatrix} (\psi^\alpha + \mu^\alpha + \omega^\alpha)E \\ (\mu^\alpha + \sigma^\alpha + \gamma_S^\alpha)I_S - \delta\omega^\alpha E \\ (\mu^\alpha + \sigma^\alpha + \gamma_A^\alpha)I_S - (1-\delta)\omega^\alpha E \\ \mu_P^\alpha P. \end{pmatrix}$$

The matrices $\mathcal{F}$ and $\mathcal{V}$ represents the rate of production of new infections and transition of new infections respectively.

Linearizing the infected subsystem about the disease-free equilibrium point, we obtain the corresponding rate of infection and infection transition rate near the equilibrium, respectively, as

$$F = \begin{pmatrix} 0 & \frac{\beta_2^\alpha b^\alpha}{\mu^\alpha} & \frac{\beta_2^\alpha b^\alpha}{\mu^\alpha} & \frac{\beta_1^\alpha b^\alpha}{\mu^\alpha} \\ 0 & 0 & 0 & 0 \\ 0 & 0 & 0 & 0 \\ 0 & \eta_A^\alpha & \eta_S^\alpha & 0 \end{pmatrix} \qquad V = \begin{pmatrix} c_1^\alpha & 0 & 0 & 0 \\ -\delta\omega^\alpha & 0 & c_2^\alpha & 0 \\ (\delta-1)\omega^\alpha & c_3^\alpha & 0 & 0 \\ 0 & 0 & 0 & \mu_P^\alpha \end{pmatrix}$$

where

$$c_1^\alpha := \psi^\alpha + \mu^\alpha + \omega^\alpha; \quad c_2^\alpha := \mu^\alpha + \sigma^\alpha + \gamma_S^\alpha; \quad c_3 := \mu^\alpha + \sigma^\alpha + \gamma_A^\alpha.$$

The basic reproduction number is the spectral radius of matrix $K = FV^{-1}$, the total production of new infections over the course of outbreak. Using symbolic computation Maple17 software,

we compute

$$K = \begin{pmatrix} \frac{\beta_2^\alpha b^\alpha \omega^\alpha \delta}{\mu^\alpha c_1^\alpha c_2^\alpha} + \frac{\beta_2^\alpha b^\alpha (1-\delta)\omega^\alpha}{\mu^\alpha c_1^\alpha c_3^\alpha} & \frac{\beta_2^\alpha b^\alpha}{\mu^\alpha c_2^\alpha} & \frac{\beta_2^\alpha b^\alpha}{\mu^\alpha c_3^\alpha} & \frac{\beta_1^\alpha b^\alpha}{\mu^\alpha \mu_P^\alpha} \\ 0 & 0 & 0 & 0 \\ 0 & 0 & 0 & 0 \\ \frac{\eta_S^\alpha \omega^\alpha \delta}{c_1^\alpha c_2^\alpha} + \frac{\eta_A^\alpha \omega^\alpha (1-\delta)}{c_1^\alpha c_3^\alpha} & \frac{\eta_S^\alpha}{c_2^\alpha} & \frac{\eta_A^\alpha}{c_3^\alpha} & 0 \end{pmatrix}.$$

As suggested by [81], the above matrix can be further reduced to a 2×2 matrix through a certain transformation matrix $\mathbb{E}$, while still preserving the dominant eigenvalue. It is immediate from matrix F that such a transformation matrix is $\mathbb{E} = \begin{pmatrix} 1 & 0 \\ 0 & 0 \\ 0 & 0 \\ 0 & 1 \end{pmatrix}$. Let us now define the *reduced* matrix K_S by

$$K_S = \mathbb{E}^T K \mathbb{E} = \begin{pmatrix} \frac{\beta_2^\alpha b^\alpha \omega^\alpha \delta}{\mu^\alpha c_1^\alpha c_2^\alpha} + \frac{\beta_2^\alpha b^\alpha (1-\delta)\omega^\alpha}{\mu^\alpha c_1^\alpha c_3^\alpha} & \frac{\beta_1^\alpha b^\alpha}{\mu^\alpha \mu_P^\alpha} \\ \frac{\eta_S^\alpha \omega^\alpha \delta}{c_1^\alpha c_2^\alpha} + \frac{\eta_A^\alpha \omega^\alpha (1-\delta)}{c_1^\alpha c_3^\alpha} & 0 \end{pmatrix}.$$

Consequently, it follows that $\rho(K) = \rho(K_S) = \frac{1}{2}\Big(\text{trace}(K_S) + \sqrt{\text{trace}(K_S)^2 - 4\det(K_S)}\Big)$. Hence,

$$R_0 = \frac{\beta_2^\alpha b^\alpha \omega^\alpha \delta}{\mu^\alpha c_1^\alpha c_2^\alpha} + \frac{\beta_2^\alpha b^\alpha (1-\delta)\omega^\alpha}{\mu^\alpha c_1^\alpha c_3^\alpha} + \sqrt{\Big(\frac{\beta_2^\alpha b^\alpha \omega^\alpha \delta}{\mu^\alpha c_1^\alpha c_2^\alpha} + \frac{\beta_2^\alpha b^\alpha (1-\delta)\omega^\alpha}{\mu^\alpha c_1^\alpha c_3^\alpha}\Big)^2 + \frac{\beta_1^\alpha b^\alpha}{\mu^\alpha \mu_P^\alpha}\Big(\frac{\eta_S^\alpha \omega^\alpha \delta}{c_1^\alpha c_2^\alpha} + \frac{\eta_A^\alpha \omega^\alpha (1-\delta)}{c_1^\alpha c_3^\alpha}\Big)}.$$

The following theorem, which is immediate from [82, Theorem 2], elucidate the importance of the basic reproduction number R_0 derived above.

Theorem 4.4. *The disease-free equilibrium point* $(b^\alpha/\mu^\alpha, 0, 0, 0, 0, 0)$ *of the fractional model* (6) *is locally asymptotically stable (LAS) if* $R_0 < 1$, *and unstable if* $R_0 > 1$.

The above theorem 4.4 implies that the fractional order epidemic model (6) is controllable through appropriate control measures (via the parameters α_1 and α_2) such as minimizing contact with infectious individuals as well as shedding of the virus pathogen by infected individuals to the environment.

4.2.1 Global stability

We establish the global stability of the fractional model (6) in the sense of Ulam-Hyers [**?**]. The Ulam-Hyers stability has been an active research area since it was first introduced by Ulam in 1940 at Winscosing University and a follow-up work by Rassias in the years between 1982 and 1998. Recently the authors in [66] established Ulam-Hyers stability of a nonlinear fractional model of Covid-19 pandemic.

For clarity of the discussion that follows, let us introduce the inequality given by

$$|D_t^\alpha X(t) - \mathcal{K}(t, X(t))| \leq \epsilon, \quad t \in [0, b]. \tag{10}$$

We say a function $\bar{X} \in \mathcal{E}$ is a solution of (10) if and only if there exists $h \in \mathcal{E}$ satisfying

i. $|h(t)| \leq \epsilon$

ii. $D_t^\alpha \bar{X}(t) = \mathcal{K}(t, \bar{X}(t)) + h(t), \quad t \in [0, b]$.

It is important to observe that by invoking (7) and property ii. above, simple simplification yields the fact that any function $\bar{X} \in \mathcal{E}$ satisfying (10) also satisfies the integral inequality

$$\Big|\bar{X}(t) - \bar{X}(0) - \frac{1}{\Gamma(\alpha)}\int_0^t (t-\tau)^{\alpha-1}\mathcal{K}(\tau, \bar{X}(\tau))\Big| \leq \Omega\epsilon \tag{11}$$

Definition 4.5. *The fractional order model* (6) *(and equivalently* (5)*) is Ulam-Hyers stable if there exists* $C_{\mathcal{K}} > 0$ *such that for every* $\epsilon > 0$ *and for each solution* $\bar{X} \in \mathcal{E}$ *satisfying* (10)*, there exists a solution* $X \in \mathcal{E}$ *of* (6) *with*

$$||\bar{X}(t) - X(t)||_{\mathcal{E}} \leq C_{\mathcal{K}}\epsilon, \quad t \in [0, b].$$

Definition 4.6. *The fractional order model* (6) *(and equivalently* (5)*) is said to be generalized Ulam-Hyers stable if there exists a continuous function* $\phi_{\mathcal{K}} : \mathbb{R}^+ \to \mathbb{R}^+$ *with* $\phi_{\mathcal{K}}(0) = 0$*, such that, for each solution* $\bar{X} \in \mathcal{E}$ *of* (10)*, there exists a solution* $X \in \mathcal{E}$ *of* (6) *such that*

$$||\bar{X}(t) - X(t)||_{\mathcal{E}} \leq \phi_{\mathcal{K}}\epsilon, \quad t \in [0, b].$$

We now present our result on stability of the fractional order model.

Theorem 4.7. *Let the hypothesis and result of Lemma 4.2 hold,* $\Omega = \frac{b^\alpha}{\Gamma(\alpha+1)}$ *and* $1 - \Omega L_{\mathcal{K}} > 0$*. Then, the fractional order model* (6) *(and equivalently* (5)*) is Ulam-Hyers stable and consequently generalized Ulam-Hyers stable.*

Proof. Let X be a unique solution of (6) guaranteed by Theorem 4.3; $\bar{X}$ satisfies (10). Then recalling the expressions (7), (11), we have for $\epsilon > 0, t \in [0, b]$ that

$$\begin{aligned}
||\bar{X} - X||_{\mathcal{E}} &= \sup_{t\in[0,b]} |\bar{X}(t) - X(t)| \\
&= \sup_{t\in[0,b]} \left|\bar{X}(t) - X_0 - \frac{1}{\Gamma(\alpha)}\int_0^t (t-\tau)^{\alpha-1}\mathcal{K}(\tau, X(\tau))\mathrm{d}\tau\right| \\
&\leq \sup_{t\in[0,b]} \left|\bar{X}(t) - \bar{X}_0 - \frac{1}{\Gamma(\alpha)}\int_0^t (t-\tau)^{\alpha-1}\mathcal{K}(\tau, \bar{X}(\tau))\mathrm{d}\tau\right| \\
&\quad + \sup_{t\in[0,b]} \frac{1}{\Gamma(\alpha)}\int_0^t (t-\tau)^{\alpha-1}|\mathcal{K}(\tau, \bar{X}(\tau)) - \mathcal{K}(\tau, X(\tau))|\mathrm{d}\tau \\
&\leq \Omega\epsilon + \frac{L_{\mathcal{K}}}{\Gamma(\alpha)} \sup_{t\in[0,b]} \int_0^t (t-\tau)^{\alpha-1}|\bar{X}(\tau) - X(\tau)|\mathrm{d}\tau \\
&\leq \Omega\epsilon + \Omega L_{\mathcal{K}}||\bar{X} - X||_{\mathcal{E}}
\end{aligned}$$

from which we obtain $||\bar{X} - X||_{\mathcal{E}} \leq C_{\mathcal{K}}\epsilon$ where $C_{\mathcal{K}} = \frac{\Omega}{1-\Omega L_{\mathcal{K}}}$. □

5 Numerical simulation and discussion

This section provides some illustrative numerical simulations to explain the dynamical behavior of the Caputo fractional-order deterministic nonlinear COVID-19 mathematical model. The numerical solution of a nonlinear mathematical model using the appropriate iterative scheme is very important in mathematical modeling. For this purpose, we have used the Adams-type predictor-corrector iterative scheme constructed in [83, 84] to solve fractional-order differential equations. The method relies on equivalent integral formulation of our fractional model (5) written in the form (6). Consider a uniform discretization of $[0, b]$ given by $t_n = nh$, $n = 0, 1, 2, \ldots, N$ where $0 < h = b/n$ denote the step size. Now, given any approximation $X_h(t_i) \approx X(t_i)$, we obtain the next approximation $X_h(t_{i+1})$ using the Adams-type predictor-corrector iterative scheme as follows;

Predictor:

$$X_h^p(t_{n+1}) = \sum_{k=0}^{\lceil\alpha\rceil-1} \frac{t_{n+1}^k}{k!}X_0^k + \frac{1}{\Gamma(\alpha)}\sum_{i=0}^{n} b_{i,n+1}\mathcal{K}(t_i, X_h(t_i))$$

Corrector:

$$X_h(t_{n+1}) = \sum_{k=0}^{\lceil\alpha\rceil-1} \frac{t_{n+1}^k}{k!} X_0^k + \frac{h^\alpha}{\Gamma(\alpha+2)} \mathcal{K}(t_{i+1}, X_h^p(t_{i+1})) + \frac{h^\alpha}{\Gamma(\alpha+2)} \sum_{i=0}^{n} a_{i,n+1} \mathcal{K}(t_i, X_h(t_i))$$

with

$$a_{i,n+1} = \begin{cases} n^{\alpha+1} - (n-\alpha)(n+1)^\alpha, & \text{if } i = 0 \\ (n-i+2)^{\alpha+1} + (n-i)^{\alpha+1} - 2(n-i+1)^{\alpha+1}, & \text{if } 1 \le i \le n \\ 1, & \text{if } i = n+1 \end{cases}$$

and

$$b_{i,n+1} = \frac{h^\alpha}{\alpha} \big[(n-i+1)^\alpha - (n-i)^\alpha\big].$$

For varying values of the derivative order α, the dynamics of the fractional order model are presented in Figures 4 below. We have used the model parameters in Table 1 as reported in [72] and initial data $S(0) = 93000, E(0) = 1000, I_A(0) = 50, I_S(0) = 50, R(0) = 0, P(0) = 500$. For $\alpha = 1$, coinciding with the integer-order model, the obtained dynamics is consistent with those reported in Section 3 and [72]. In Figures 4, effect of the fractional order α on disease progression are demonstrated. Furthermore, the basic reproduction number of the disease-free equilibrium point $\Sigma = \left(\frac{b^\alpha}{\mu^\alpha}, 0, 0, 0, 0, 0\right) = (1.9861, 0, 0, 0, 0, 0,)$ for $\alpha = 0.5$ was computed as $R_0 = 0.87831 < 1$, showing the fulfillment of the necessary and sufficient conditions for local asymptotic stability of the disease-free equilibrium of Theorem 4.4. We also found out that for fractional orders considered namely $\alpha \in \{1, 0.9, 0.8, 0.7\}$, and with new infection rates $\alpha_1 = \alpha_2 = 0.1$, the corresponding computed $R_0 \in [0.90850, 0.82590]$ showing that the COVID-19 pandemic is controllable and will effectively die out as long as there is compliance with social distancing/lockdown regulations, and if infectious and infected individuals are appropriately quarantined, thereby preventing contamination of the environment through virus shedding.

Recall that the constants α_1 and α_2 represent the proportion of interaction with the infectious environment and infectious individuals respectively. Consider a scenario of a contaminated environment $\alpha_1 = 0.05$ where there is higher chances of contracting COVID-19 through the environment than through infectious individuals I_A or I_S, ($\alpha_1 = 0.1$). In this situation, a rapid decline in the susceptible population is noticeable in figure 6a during the first ten days. This is expected as more people get exposed through virus-laden environment, explaining the rapid rise in the exposed population and the infected population within the same time period, figure 6b, 6c and figure 6d. In comparison with other scenarios, namely $\alpha_2 = 0.05, \alpha_1 = 0.1$ where there is higher risk of contracting COVID-19 virus through contacts with infectious individuals than through the environment; and $\alpha_2 = 0.1, \alpha_1 = 0.1$ depicting generally low infection rate from both sources, the number of exposed, asymptomatic infectious and symptomatic infectious populations peaked in the former.

6 Conclusion

We have proposed a fractional order epidemic model for COVID-19 infection dynamics based on the integer-order model of [72] incorporating social distancing measures and interaction with environment. Qualitative analysis of both integer order and fractional order models were carried out. In particular, we established the well-posedness of the fractional model via the Banach fixed point theorem. Using the concept of next-generation matrices for computing basic reproduction number R_0, local asymptotic stability of the fractional model was proved. Furthermore, we showed the global stability of the model in the sense of Ulam-Hyer stability criteria. Numerical simulations confirmed the established properties of the proposed model, and more importantly elucidated the need for compliance with regulations on basic preventive measures such as social

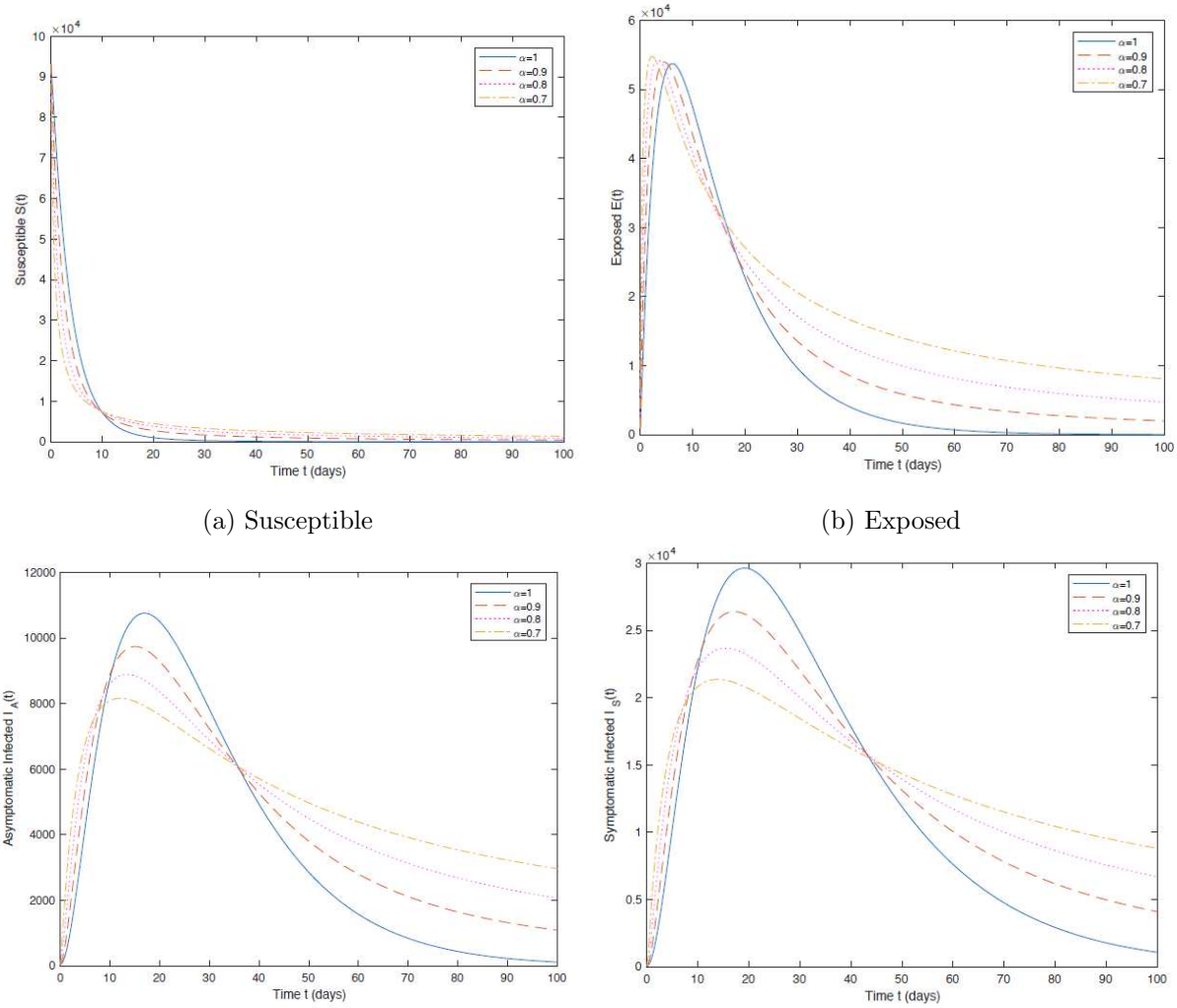

(a) Susceptible

(b) Exposed

(c) Asymptomatic Infected

(d) Symptomatic Infected

Figure 4: Population dynamics of the fractional model for $\alpha \in \{1, 0.9, 0.8, 0.7\}$ labelled respectively a-d.

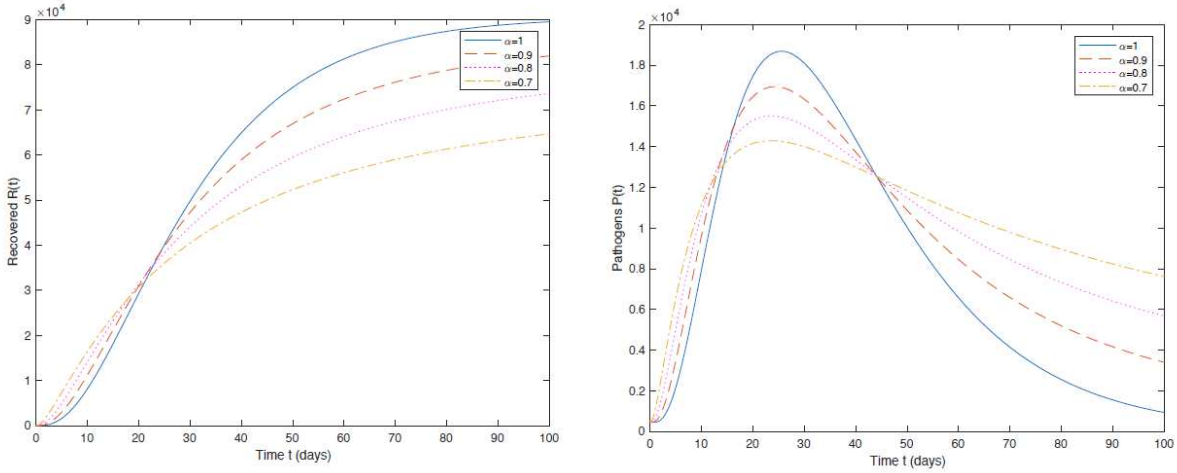

(a) Recovered (b) Pathogens

Figure 5: Recovered and Pathogens population dynamics of the fractional model for $\alpha \in \{1, 0.9, 0.8, 0.7\}$ labelled respectively (a), (b) respectively.

distancing, quarantining of infectious and infected individuals, and frequent hand washing to rid the population of the deadly virus.

Declarations of conflict of interests

The authors declared no potential conflicts of interest with respect to the research, authorship, and/or publication of this article.

References

[1] Carlos Castillo-Chavez and Baojun Song. Dynamical models of tuberculosis and their applications. *Math Biosci Eng*, 1(2):361, 2004.

[2] Oluwaseun Sharomi, Chandra N Podder, Abba B Gumel, and Baojun Song. Mathematical analysis of the transmission dynamics of hiv/tb coinfection in the presence of treatment. *Math Biosci Eng*, 5(1):145, 2008.

[3] Fred Brauer. The kermack–mckendrick epidemic model revisited. *Math Biosci*, 198(2):119–131, 2005.

[4] Herbert W Hethcote. The mathematics of infectious diseases. *SIAM review*, 42(4):599–653, 2000.

[5] Wei-min Liu, Herbert W Hethcote, and Simon A Levin. Dynamical behavior of epidemiological models with nonlinear incidence rates. *J Math Biol*, 25(4):359–380, 1987.

[6] Novi Reandy Sasmita, Muhammad Ikhwan, Suyanto Suyanto, and Virasakdi Chongsuvivatwong. Optimal control on a mathematical model to pattern the progression of coronavirus disease 2019 (covid-19) in indonesia. *Glob Health Res Policy*, 5(1):1–12, 2020.

[7] Eugene B Postnikov. Estimation of covid-19 dynamics "on a back-of-envelope": Does the simplest sir model provide quantitative parameters and predictions? *Chaos, Solitons & Fractals*, 135:109841, 2020.

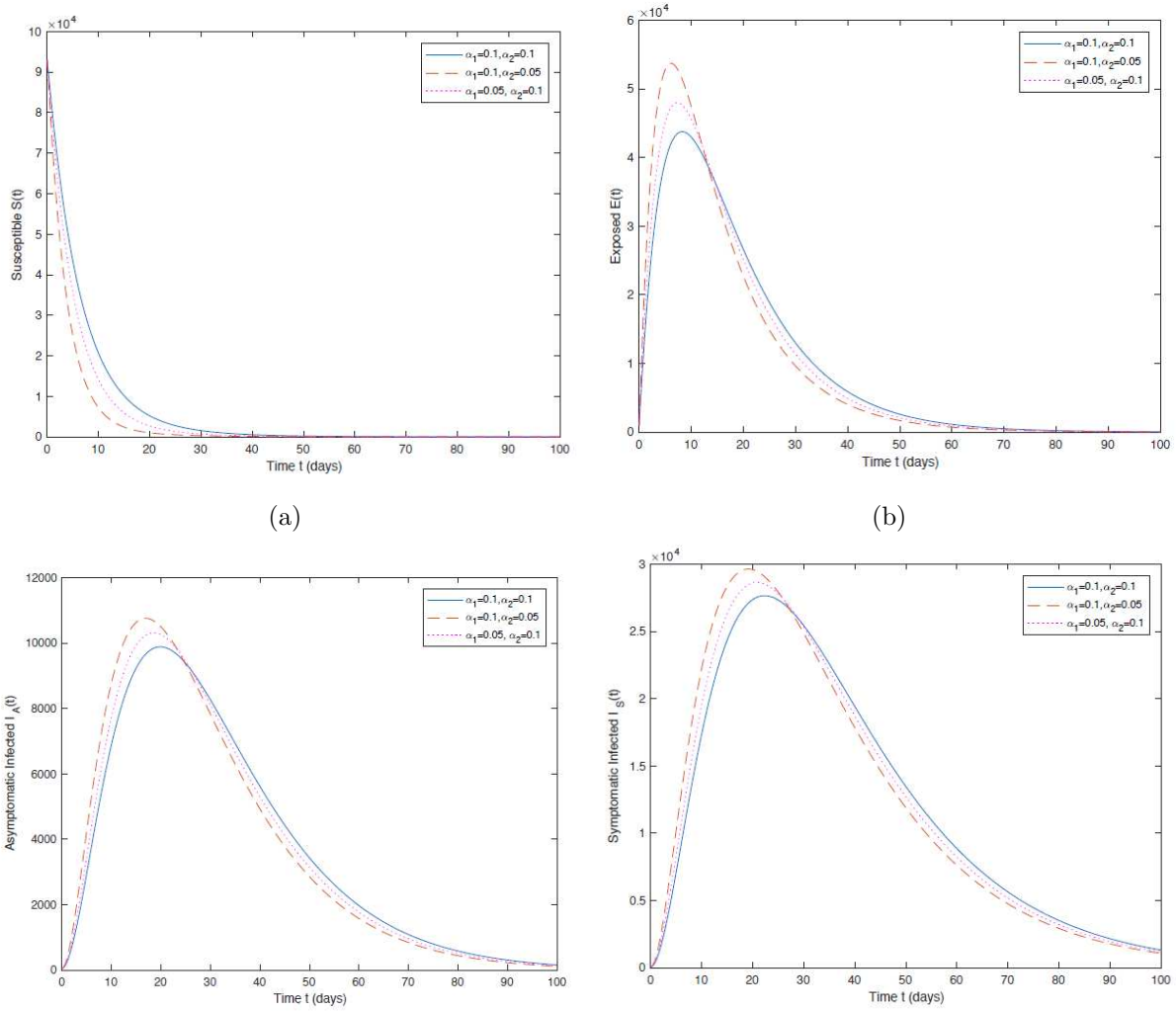

Figure 6: Effect of new rate of infections through the environment (α_1) and through contact with infected individuals (α_2) on population dynamics

[8] Giulia Giordano, Franco Blanchini, Raffaele Bruno, Patrizio Colaneri, Alessandro Di Filippo, Angela Di Matteo, and Marta Colaneri. Modelling the covid-19 epidemic and implementation of population-wide interventions in italy. *Nat Med*, pages 1–6, 2020.

[9] Qianying Lin, Shi Zhao, Daozhou Gao, Yijun Lou, Shu Yang, Salihu S Musa, Maggie H Wang, Yongli Cai, Weiming Wang, Lin Yang, et al. A conceptual model for the outbreak of coronavirus disease 2019 (covid-19) in wuhan, china with individual reaction and governmental action. *Int J Infect Dis*, 2020.

[10] Xinmiao Rong, Liu Yang, Huidi Chu, and Meng Fan. Effect of delay in diagnosis on transmission of covid-19. *Math Biosci Eng*, 17(3):2725–2740, 2020.

[11] D Okuonghae and A Omame. Analysis of a mathematical model for covid-19 population dynamics in lagos, nigeria. *Chaos, Solitons & Fractals*, 139:110032, 2020.

[12] Benjamin Ivorra, Miriam Ruiz Ferrández, Maria Vela-Pérez, and AM Ramos. Mathematical modeling of the spread of the coronavirus disease 2019 (covid-19) taking into account the undetected infections. the case of china. *Commun Nonlinear Sci Numer Simul*, 88:105303, 2020.

[13] Joshua Kiddy K Asamoah, Mark A Owusu, Zhen Jin, FT Oduro, Afeez Abidemi, and Esther Opoku Gyasi. Global stability and cost-effectiveness analysis of covid-19 considering the impact of the environment: using data from ghana. *Chaos, Solitons & Fractals*, 140:110103, 2020.

[14] Abdul-Rahman J Mumbu and Alfred K Hugo. Mathematical modelling on covid-19 transmission impacts with preventive measures: a case study of tanzania. *J Biol Dyn*, 14(1):748–766, 2020.

[15] Igor Podlubny. *Fractional differential equations: an introduction to fractional derivatives, fractional differential equations, to methods of their solution and some of their applications*. Elsevier, 1998.

[16] Ivo Petráš. *Fractional-order nonlinear systems: modeling, analysis and simulation*. Springer Science & Business Media, 2011.

[17] Carla MA Pinto and Ana RM Carvalho. A latency fractional order model for hiv dynamics. *J Comp Appl Math*, 312:240–256, 2017.

[18] Yongsheng Ding and Haiping Ye. A fractional-order differential equation model of hiv infection of cd4+ t-cells. *Math Comput Model*, 50(3-4):386–392, 2009.

[19] Parvaiz Ahmad Naik, Kolade M Owolabi, Mehmet Yavuz, and Jian Zu. Chaotic dynamics of a fractional order hiv-1 model involving aids-related cancer cells. *Chaos, Solitons & Fractals*, 140:110272, 2020.

[20] Carla MA Pinto and Ana RM Carvalho. The role of synaptic transmission in a hiv model with memory. *Appl Math Comput*, 292:76–95, 2017.

[21] Zain Ul Abadin Zafar, Kashif Rehan, and M Mushtaq. Hiv/aids epidemic fractional-order model. *J Diff Equ Appl*, 23(7):1298–1315, 2017.

[22] Endrik Mifta Shaiful, Mohammad Imam Utoyo, et al. A fractional-order model for hiv dynamics in a two-sex population. *Int J Math Math Sci*, 2018, 2018.

[23] AAM Arafa, SZ Rida, and M Khalil. Fractional modeling dynamics of hiv and cd4+ t-cells during primary infection. *Nonlinear Biomed Phys*, 6(1):1, 2012.

[24] AAM Arafa, SZ Rida, and M Khalil. A fractional-order model of hiv infection: Numerical solution and comparisons with data of patients. *Int J Biomath*, 7(04):1450036, 2014.

[25] Cristiana J Silva and Delfim FM Torres. Stability of a fractional hiv/aids model. *Math Comput Simul*, 164:180–190, 2019.

[26] Muhammad Altaf Khan, Hafidz Putra Odinsyah, et al. Fractional model of hiv transmission with awareness effect. *Chaos, Solitons & Fractals*, 138:109967, 2020.

[27] Hatıra Günerhan, Hemen Dutta, Mustafa Ali Dokuyucu, and Waleed Adel. Analysis of a fractional hiv model with caputo and constant proportional caputo operators. *Chaos, Solitons & Fractals*, 139:110053, 2020.

[28] Ahmet Gökdoğan, Ahmet Yildirim, and Mehmet Merdan. Solving a fractional order model of hiv infection of cd4+ t cells. *Math Comput Model*, 54(9-10):2132–2138, 2011.

[29] P Tamilalagan, S Karthiga, and P Manivannan. Dynamics of fractional order hiv infection model with antibody and cytotoxic t-lymphocyte immune responses. *J Comput Appl Math*, 382:113064.

[30] Ana RM Carvalho, Carla MA Pinto, and Dumitru Baleanu. Hiv/hcv coinfection model: a fractional-order perspective for the effect of the hiv viral load. *Adv Differ Equ*, 2018(1):1–22, 2018.

[31] NH Sweilam, SM AL-Mekhlafi, ZN Mohammed, and D Baleanu. Optimal control for variable order fractional hiv/aids and malaria mathematical models with multi-time delay. *Alex Eng J*, 59(5):3149–3162, 2020.

[32] Weronika Wojtak, Cristiana J Silva, and Delfim FM Torres. Uniform asymptotic stability of a fractional tuberculosis model. *Math Model Nat Phenom*, 13(1):9, 2018.

[33] Ihsan Ullah, Saeed Ahmad, Mati ur Rahman, and Muhammad Arfan. Investigation of fractional order tuberculosis (tb) model via caputo derivative. *Chaos, Solitons & Fractals*, page 110479, 2020.

[34] Abdon Atangana and Sania Qureshi. Mathematical modeling of an autonomous nonlinear dynamical system for malaria transmission using caputo derivative. *Fractional Order Analysis: Theory, Methods and Applications*, pages 225–252, 2020.

[35] Carla MA Pinto and JA Tenreiro Machado. Fractional model for malaria transmission under control strategies. *Comput Math Appl*, 66(5):908–916, 2013.

[36] E Okyere, FT Oduro, SK Amponsah, IK Dontwi, and NK Frempong. Fractional order malaria model with temporary immunity. *arXiv preprint arXiv:1603.06416*, 2016.

[37] Adem Kilicman et al. A fractional order sir epidemic model for dengue transmission. *Chaos, Solitons & Fractals*, 114:55–62, 2018.

[38] Kai Diethelm. A fractional calculus based model for the simulation of an outbreak of dengue fever. *Nonlinear Dyn*, 71(4):613–619, 2013.

[39] Hamed Al-Sulami, Moustafa El-Shahed, Juan J Nieto, and Wafa Shammakh. On fractional order dengue epidemic model. *Math Probl Eng*, 2014, 2014.

[40] MA Khan, Arshad Khan, A Elsonbaty, and AA Elsadany. Modeling and simulation results of a fractional dengue model. *Eur Phys J Plus*, 134(8):379, 2019.

[41] R Rakkiyappan, V Preethi Latha, and Fathalla A Rihan. A fractional-order model for zika virus infection with multiple delays. *Complexity*, 2019, 2019.

[42] Muhammad Altaf Khan, Saif Ullah, and Muhammad Farhan. The dynamics of zika virus with caputo fractional derivative. *AIMS Math*, 4(1):134–146, 2019.

[43] V Preethi Latha, Fathalla A Rihan, R Rakkiyappan, and G Velmurugan. A fractional-order delay differential model for ebola infection and cd8+ t-cells response: stability analysis and hopf bifurcation. *Int J Biomath*, 10(08):1750111, 2017.

[44] Ivan Area, Hanan Batarfi, Jorge Losada, Juan J Nieto, Wafa Shammakh, and Ángela Torres. On a fractional order ebola epidemic model. *Adv Differ Equ*, 2015(1):278, 2015.

[45] Thomas Wetere Tulu, Boping Tian, and Zunyou Wu. Modeling the effect of quarantine and vaccination on ebola disease. *Adv Differ Equ*, 2017(1):1–14, 2017.

[46] SM Salman and AM Yousef. On a fractional-order model for hbv infection with cure of infected cells. *Journal of the Egyptian Mathematical Society*, 25(4):445–451, 2017.

[47] Moussa Bachraoui, Khalid Hattaf, and Noura Yousfi. Dynamics of a fractional order hbv infection model with capsids and ctl immune response. *Commun. Math. Biol. Neurosci.*, 2019:Article–ID, 2019.

[48] LC Cardoso, FLP Dos Santos, and RF Camargo. Analysis of fractional-order models for hepatitis b. *Comput Appl Math*, 37(4):4570–4586, 2018.

[49] Yongmei Su, Sinuo Liu, Shurui Song, Xiaoke Li, and Yongan Ye. Stability analysis and clinic phenomenon simulation of a fractional-order hbv infection model. *Complexity*, 2020, 2020.

[50] Ruiqing Shi, Ting Lu, and Cuihong Wang. Dynamic analysis of a fractional-order model for hepatitis b virus with holling ii functional response. *Complexity*, 2019, 2019.

[51] Jaouad Danane, Karam Allali, and Zakia Hammouch. Mathematical analysis of a fractional differential model of hbv infection with antibody immune response. *Chaos, Solitons & Fractals*, 136:109787, 2020.

[52] HAA El-Saka. Backward bifurcations in fractional-order vaccination models. *Journal of the Egyptian Mathematical Society*, 23(1):49–55, 2015.

[53] Mohammad Javidi and Bashir Ahmad. A study of a fractional-order cholera model. *Appl Math Info Sci*, 8(5):2195, 2014.

[54] Cláudia Torres Codeço. Endemic and epidemic dynamics of cholera: the role of the aquatic reservoir. *BMC Infectious diseases*, 1(1):1, 2001.

[55] Cruz Vargas-De-León. Volterra-type lyapunov functions for fractional-order epidemic systems. *Commun Nonlinear Sci Numer Simul*, 24(1-3):75–85, 2015.

[56] Elif Demirci. A fractional order model for obesity epidemic in a non-constant population. *Adv Differ Equ*, 2017(1):79, 2017.

[57] Nuri ÖZalp and Elif Demirci. A fractional order seir model with vertical transmission. *Math Comput Model*, 54(1-2):1–6, 2011.

[58] Tridip Sardar, Sourav Rana, Sabyasachi Bhattacharya, Kamel Al-Khaled, and Joydev Chattopadhyay. A generic model for a single strain mosquito-transmitted disease with memory on the host and the vector. *Math Biosci*, 263:18–36, 2015.

[59] Damian Craiem, Francisco J Rojo, Jose Miguel Atienza, Ricardo L Armentano, and Gustavo V Guinea. Fractional-order viscoelasticity applied to describe uniaxial stress relaxation of human arteries. *Phy Med Bio*, 53(17):4543, 2008.

[60] Paris Perdikaris and George Em Karniadakis. Fractional-order viscoelasticity in one-dimensional blood flow models. *Ann Biomed Eng*, 42(5):1012–1023, 2014.

[61] E Ahmed and AS Elgazzar. On fractional order differential equations model for nonlocal epidemics. *Physica A.*, 379(2):607–614, 2007.

[62] Gilberto González-Parra, Abraham J Arenas, and Benito M Chen-Charpentier. A fractional order epidemic model for the simulation of outbreaks of influenza a (h1n1). *Math Methods Appl Sci*, 37(15):2218–2226, 2014.

[63] Muhammad Awais, Fehaid Salem Alshammari, Saif Ullah, Muhammad Altaf Khan, and Saeed Islam. Modeling and simulation of the novel coronavirus in caputo derivative. *Results Phys*, 19:103588, 2020.

[64] Karthikeyan Rajagopal, Navid Hasanzadeh, Fatemeh Parastesh, Ibrahim Ismael Hamarash, Sajad Jafari, and Iqtadar Hussain. A fractional-order model for the novel coronavirus (covid-19) outbreak. *Nonlinear Dyn*, 101(1):711–718, 2020.

[65] Pushpendra Kumar and Vedat Suat Erturk. The analysis of a time delay fractional covid-19 model via caputo type fractional derivative. *Math Methods Appl Sci*, pages 10–1002.

[66] Isa Abdullahi Baba and Bashir Ahmad Nasidi. Fractional order epidemic model for the dynamics of novel covid-19. *Alex Eng J*, 2020.

[67] M. A. Bahloul, A. Chahid, and T. M. Laleg-Kirati. Fractional-order seiqrdp model for simulating the dynamics of covid-19 epidemic. *IEEE Open J Eng Med Biol*, 1:249–256, 2020.

[68] Shabir Ahmad, Aman Ullah, Qasem M Al-Mdallal, Hasib Khan, Kamal Shah, and Aziz Khan. Fractional order mathematical modeling of covid-19 transmission. *Chaos, Solitons & Fractals*, 139:110256, 2020.

[69] Idris Ahmed, Isa Abdullahi Baba, Abdullahi Yusuf, Poom Kumam, and Wiyada Kumam. Analysis of caputo fractional-order model for covid-19 with lockdown. *Adv Differ Equ*, 2020(1):1–14, 2020.

[70] Zizhen Zhang, Anwar Zeb, Oluwaseun Francis Egbelowo, and Vedat Suat Erturk. Dynamics of a fractional order mathematical model for covid-19 epidemic. *Adv Differ Equ*, 2020(1):1–16, 2020.

[71] Isaac Owusu-Mensah, Lanre Akinyemi, Bismark Oduro, and Olaniyi S Iyiola. A fractional order approach to modeling and simulations of the novel covid-19. *Adv Differ Equ*, 2020(1):1–21, 2020.

[72] Samuel Mwalili, Mark Kimathi, Viona Ojiambo, Duncan Gathungu, and Rachel Mbogo. SEIR model for COVID-19 dynamics incorporating the environment and social distancing. *BMC Research Notes*, 13(1), jul 2020.

[73] Saheed Ojo Akindeinde. A new multistage technique for approximate analytical solution of nonlinear differential equations. *Heliyon*, 6(10):e05188, 2020.

[74] Saheed Akindeinde, Samuel Adesanya, Ramosheuw S. Lebelo, and Kholeka C. Moloi. A new multistage parker-sochacki method for solving the troesch's problem. *Int J Eng Technol* , 9(2):592–601, 2020.

[75] A. Kilbas, H. Srivastava, and J. Trujillo. *Theory and Applications of Fractional Differential Equations*, volume 204. North-Holland Mathematics Studies, 2006.

[76] Z. M. Odibat and N. T. Shawagfeh. Generalized taylor's formula. *Appl Math Comput*, 186:286–293, 2007.

[77] A. McNabb. Comparison theorems for differential equations. *J Math Anal Appl*, 119:417–428, 1986.

[78] Toheeb A. Biala and Abdul Q. Khaliq. A fractional-order compartmental model for predicting the spread of the covid-19 pandemic. eprint 2007.03913, arXiv, 2020.

[79] Lin W. global existence theory and chaos control of fractional differential equations. *J. Math. Anal. Appl*, 332:709–726, 2007.

[80] A. M. A. El-Sayed. On the existence and stability of positive solution for a nonlinear fractional-order differential equation and some applications. *Alex. J. Math.*, 1:1–10, 2010.

[81] O. Diekmann, J. A. P. Heesterbeek, and M. G. Roberts. The construction of next-generation matrices for compartmental epidemic models. *J R Soc Interface*, 7(47):873–885, nov 2009.

[82] P. van den Driessche and James Watmough. Reproduction numbers and sub-threshold endemic equilibria for compartmental models of disease transmission. *Math Biosci*, 180(1):29 – 48, 2002.

[83] Kai Diethelm, Neville J Ford, and Alan D Freed. Detailed error analysis for a fractional adams method. *Numer Algorithms*, 36(1):31–52, 2004.

[84] Kai Diethelm, Neville J Ford, and Alan D Freed. A predictor-corrector approach for the numerical solution of fractional differential equations. *Nonlinear Dyn*, 29(1-4):3–22, 2002.

Figures

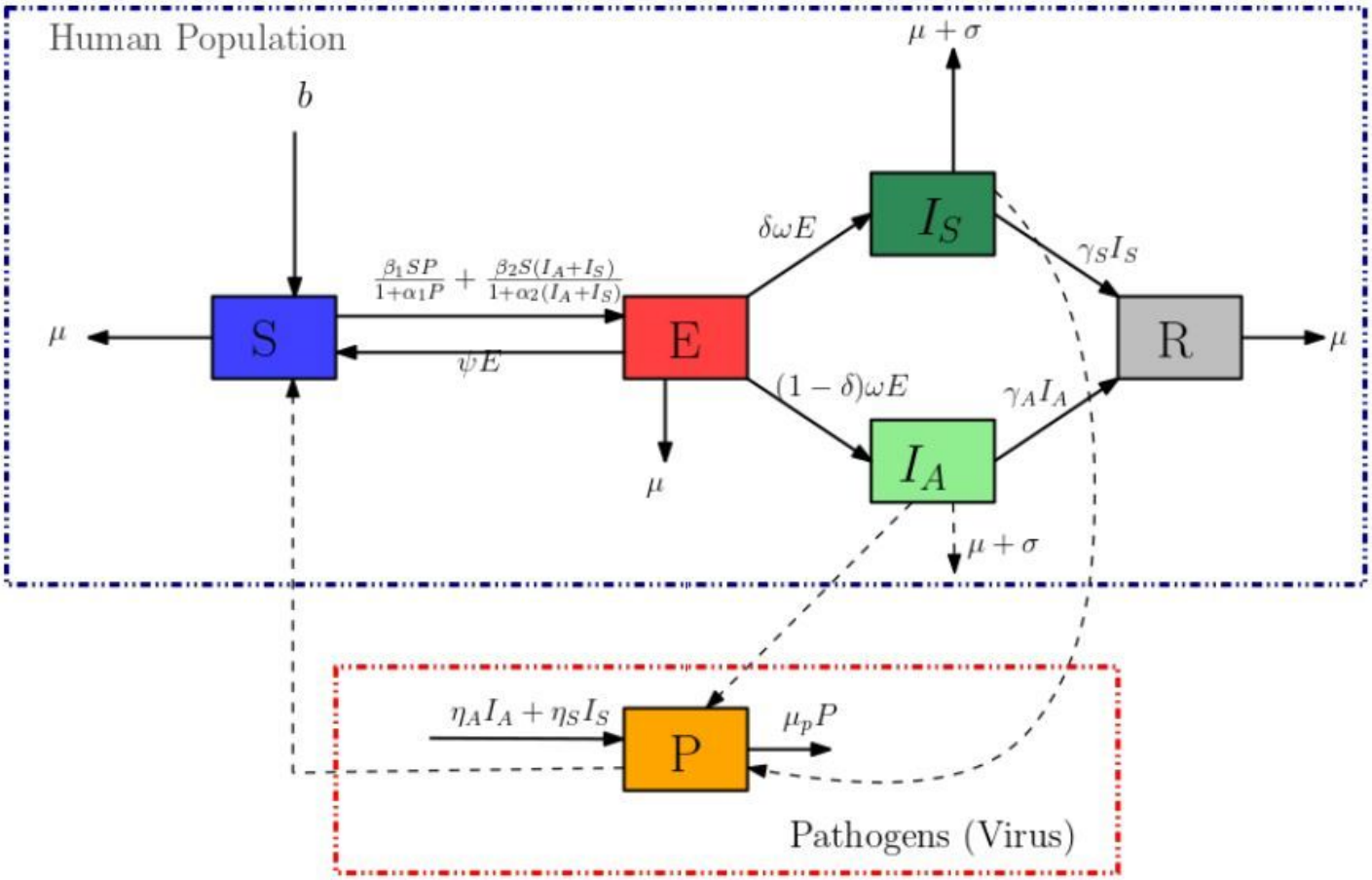

Figure 1

The SEIR-P model for COVID-19 disease dynamics

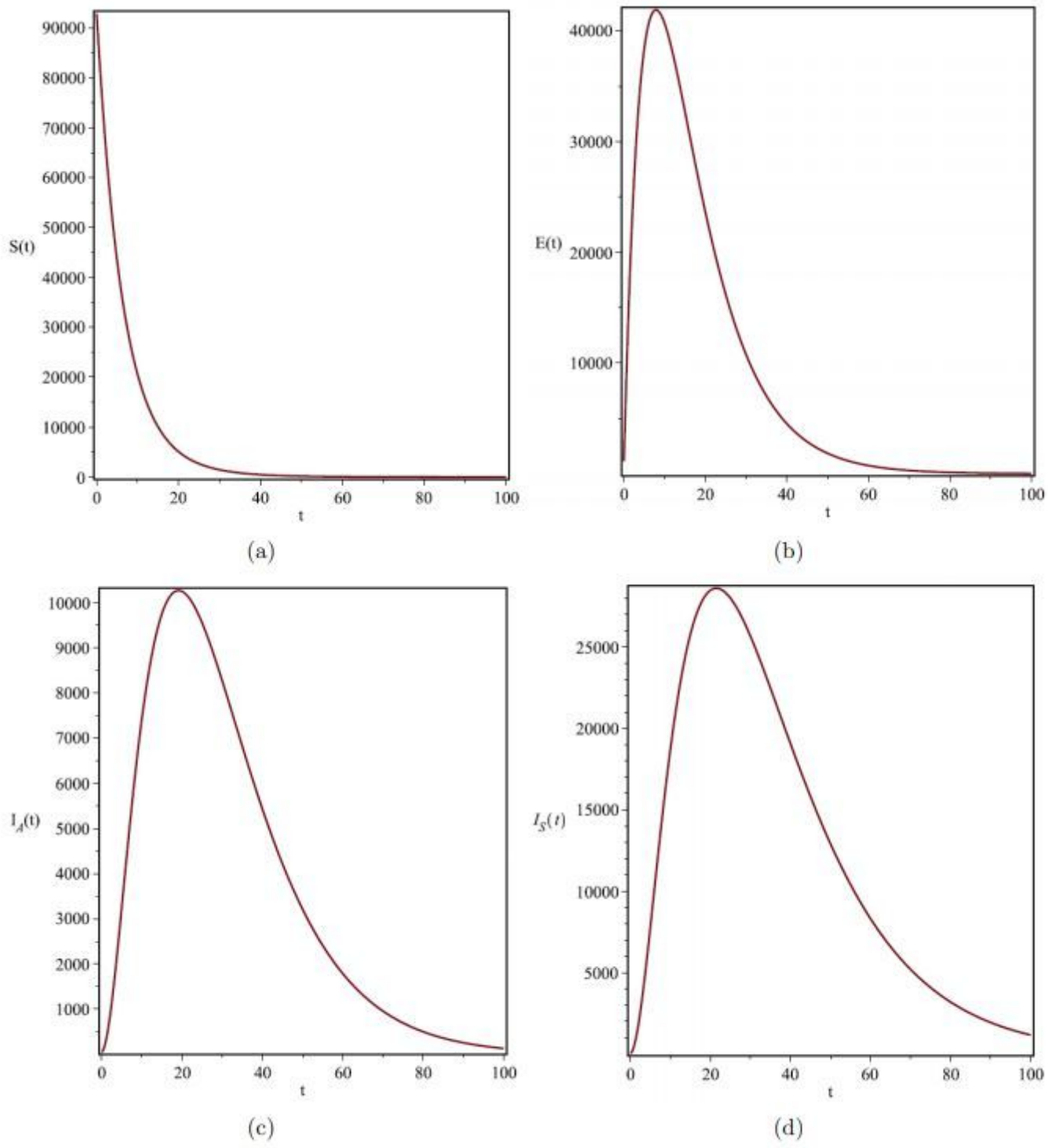

Figure 2

Disease dynamics of the integer-order model.

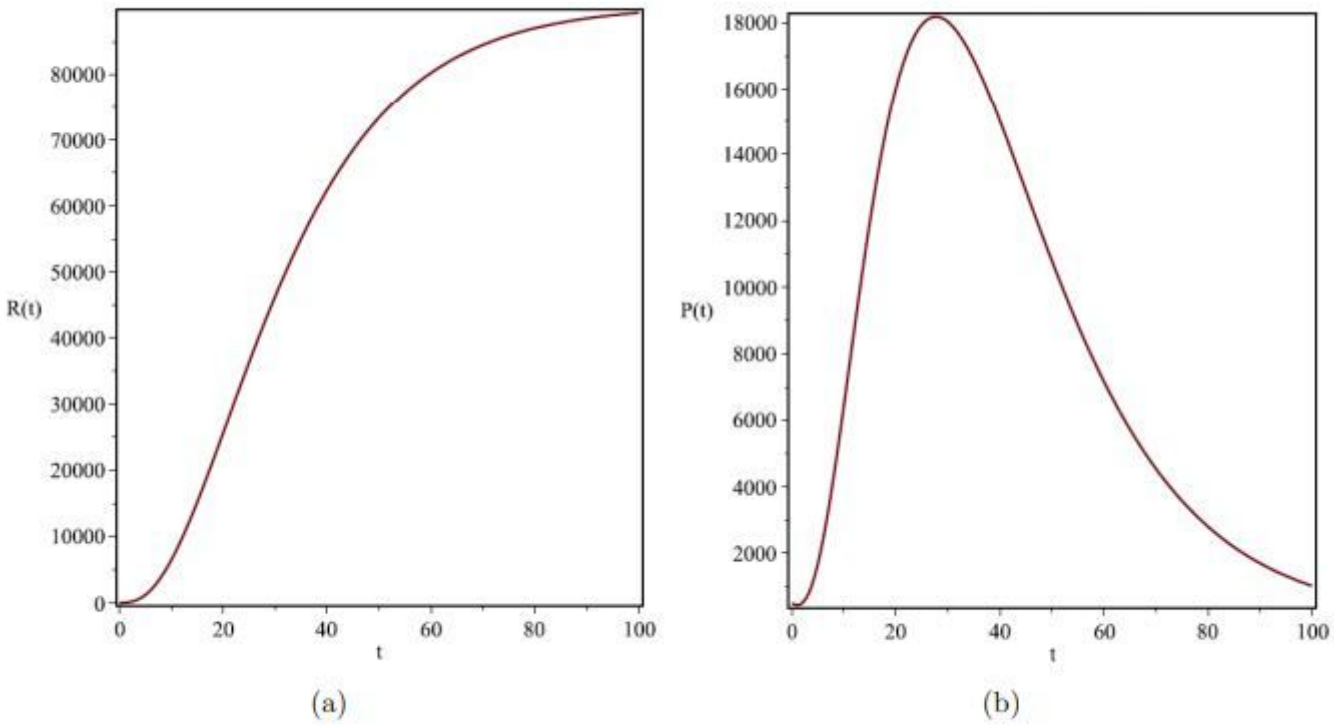

Figure 3

Disease dynamics of the integer-order model.

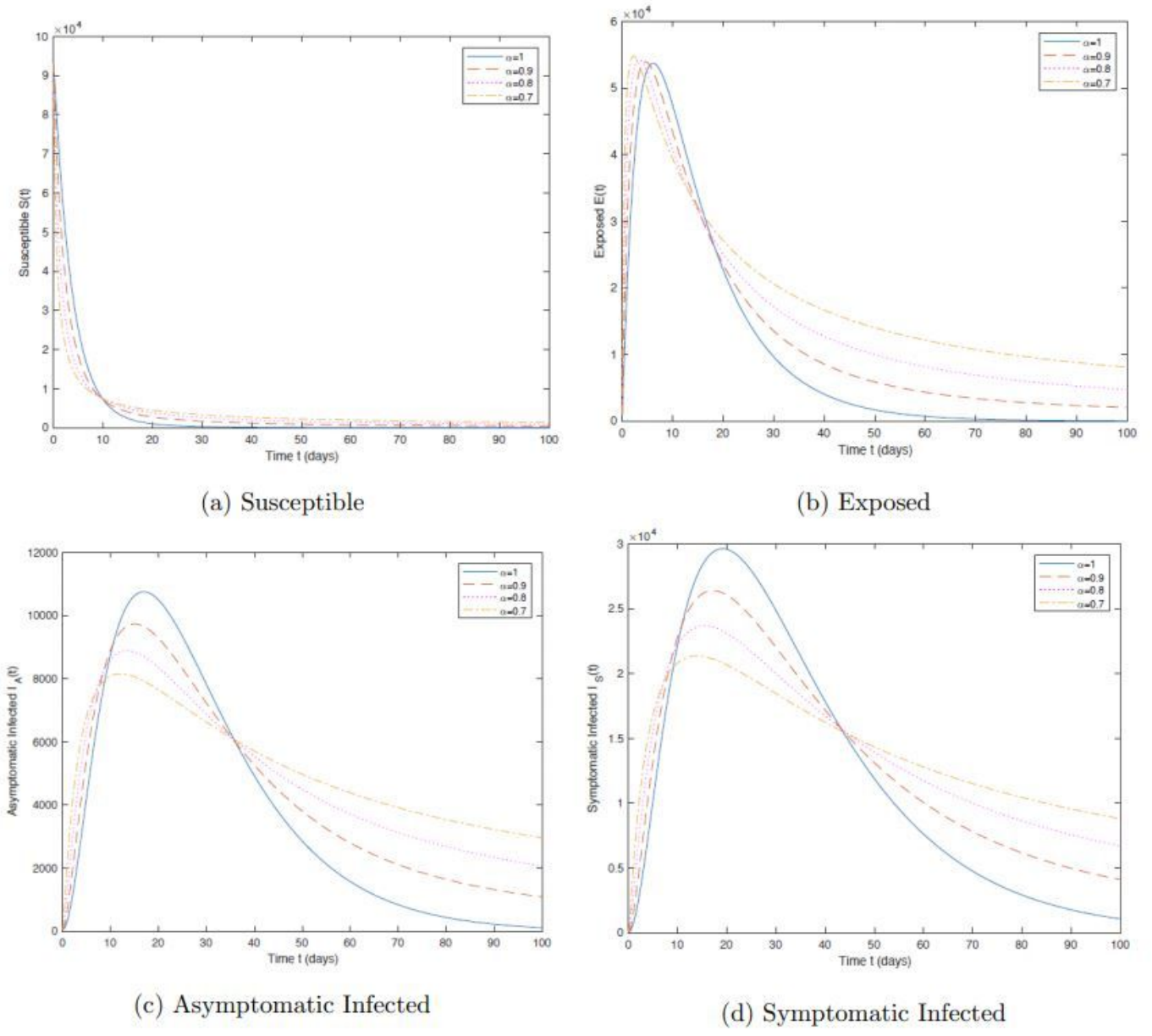

Figure 4

Population dynamics of the fractional model for 2 f1; 0:9; 0:8; 0:7g labelled respectively a-d.

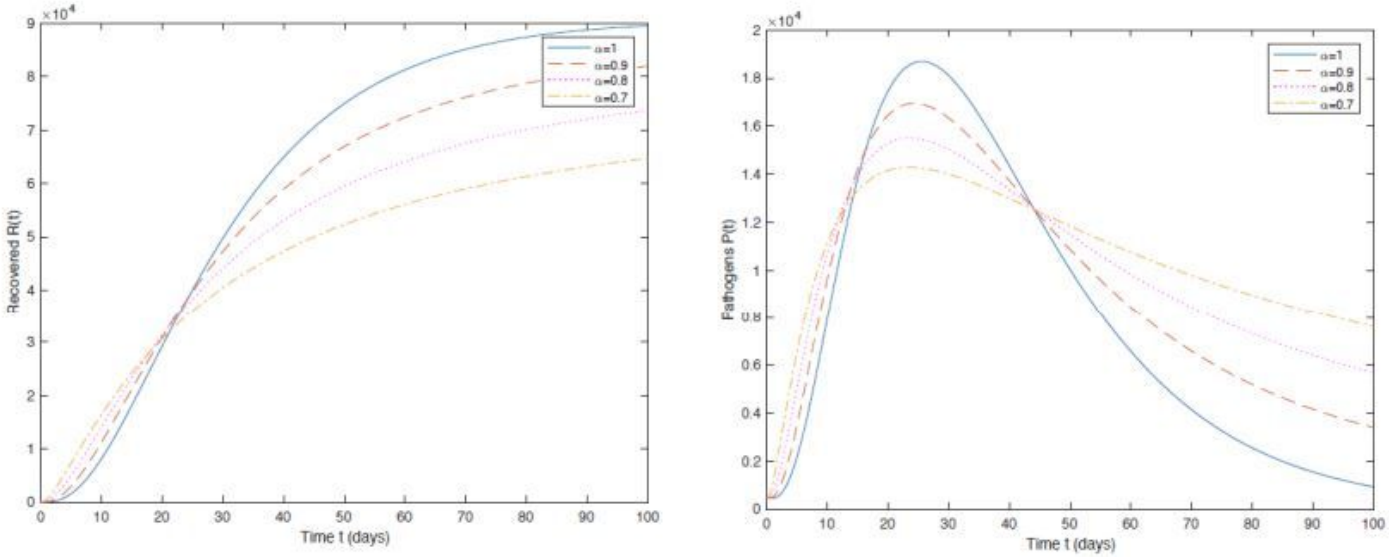

(a) Recovered (b) Pathogens

Figure 5

ecovered and Pathogens population dynamics of the fractional model for 2 f1; 0:9; 0:8; 0:7g labelled respectively (a), (b) respectively.

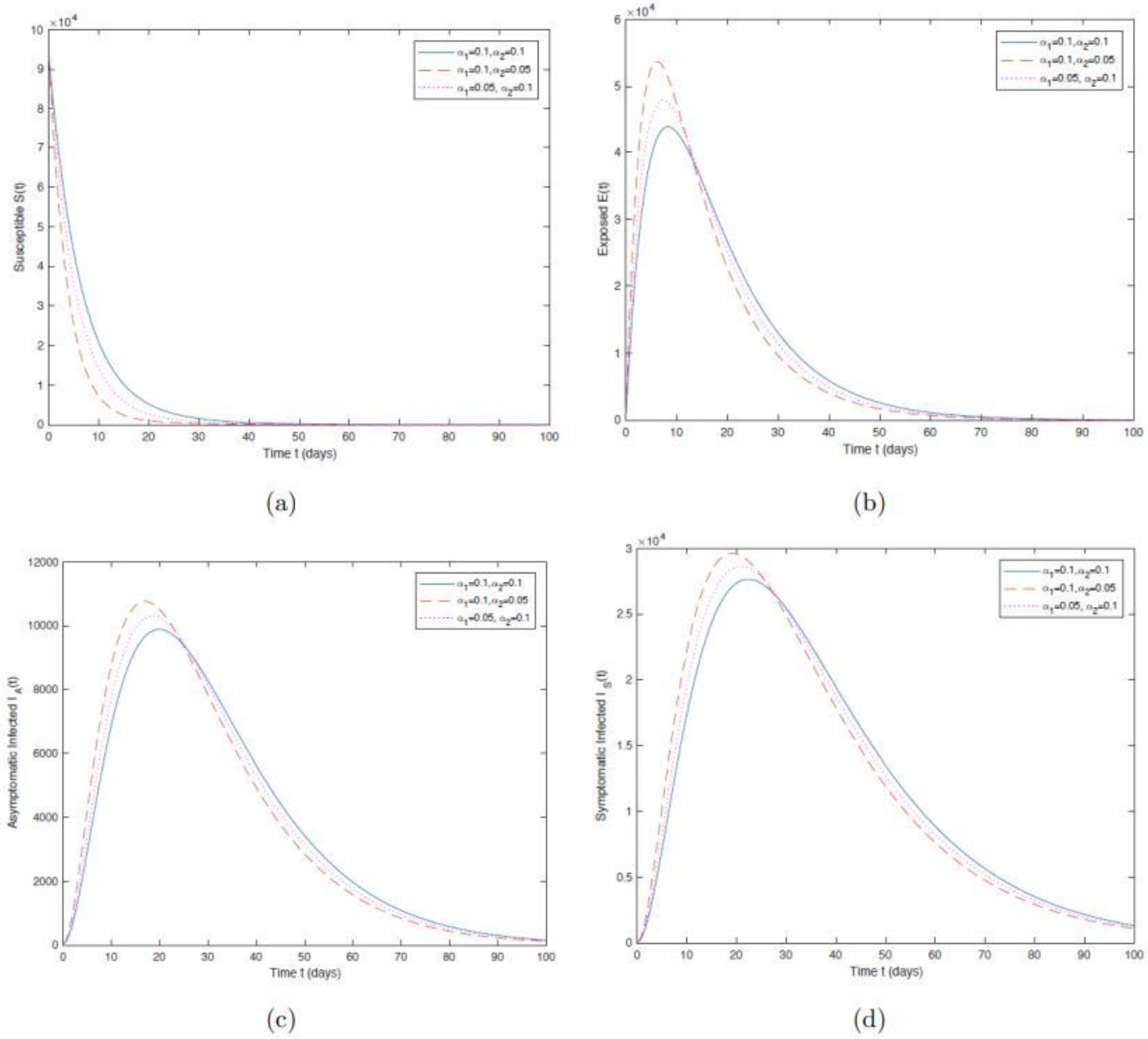

Figure 6

E□ect of new rate of infections through the environment (□1) and through contact with infected individuals (□2) on population dynamics